Hydrol. Earth Syst. Sci., 20, 4503–4524, 2016
www.hydrol-earth-syst-sci.net/20/4503/2016/
doi:10.5194/hess-20-4503-2016

Hydrology and Earth System Sciences
Open Access
EGU

Climate elasticity of streamflow revisited – an elasticity index based on long-term hydrometeorological records

Vazken Andréassian[1], **Laurent Coron**[1,a], **Julien Lerat**[2], **and Nicolas Le Moine**[3]

[1]Irstea, Hydrosystems and Bioprocesses Research Unit (HBAN), Antony, France
[2]Bureau of Meteorology, Canberra, Australia
[3]Sorbonne Universités, UPMC Univ Paris 06, CNRS, EPHE, UMR 7619 Metis, Paris, France
[a]now at: EDF-DTG, Toulouse, France

Correspondence to: Vazken Andréassian (vazken.andreassian@irstea.fr)

Received: 6 March 2015 – Published in Hydrol. Earth Syst. Sci. Discuss.: 1 April 2015
Revised: 12 July 2016 – Accepted: 23 August 2016 – Published: 10 November 2016

Abstract. We present a new method to derive the empirical (i.e., data-based) elasticity of streamflow to precipitation and potential evaporation. This method, which uses long-term hydrometeorological records, is tested on a set of 519 French catchments.

We compare a total of five different ways to compute elasticity: the reference method first proposed by Sankarasubramanian et al. (2001) and four alternatives differing in the type of regression model chosen (OLS or GLS, univariate or bivariate). We show that the bivariate GLS and OLS regressions provide the most robust solution, because they account for the co-variation of precipitation and potential evaporation anomalies. We also compare empirical elasticity estimates with theoretical estimates derived analytically from the Turc–Mezentsev formula.

Empirical elasticity offers a powerful means to test the extrapolation capacity of those hydrological models that are to be used to predict the impact of climatic changes.

1 Introduction

1.1 About hydrological elasticity

In a context of growing uncertainty regarding water resources due to climate change, simple tools able to provide robust estimates of this impact are essential to support policy and planning decisions. Streamflow elasticity is one such tool: it describes the sensitivity of the changes in streamflow related to changes in a climate variable (Schaake and Liu, 1989). $\varepsilon_{Q/X}$, the elasticity of streamflow Q to a climate variable X, is defined by the following equation:

$$\Delta Q/\overline{Q} = \varepsilon_{Q/X}\Delta X/\overline{X}, \quad (1)$$

where $\overline{Q}$ and $\overline{X}$ are the long-term average values of streamflow and the climatic variable, respectively, and the operator Δ indicates the difference between the dated and average values. $\varepsilon_{Q/X}$ is nondimensional (% / %), because it is a ratio between two relative (and thus already nondimensional) quantities. One can also define elasticity as the ratio between two absolute quantities and, provided both quantities are expressed in the same unit (for example, $\mathrm{mm\,yr^{-1}}$ for streamflow, precipitation or potential evaporation), it would still be a nondimensional ratio ($\mathrm{mm\,yr^{-1}}$ / $\mathrm{mm\,yr^{-1}}$). We will name this absolute elasticity $e_{Q/X}$, defined as

$$\Delta Q = e_{Q/X}\Delta X. \quad (2)$$

Table 1 summarizes the notations used in this paper.

1.2 Past studies on elasticity in hydrology

1.2.1 Theoretical (model-based) studies

Most of the studies on elasticity are *theoretical*, in the sense that they are based on flows simulated by a hydrological model fed with different inputs. There are many examples of such theoretical studies. Nemec and Schaake (1982) used the Sacramento model, Vogel et al. (1999) used the linear regression coefficients of annual streamflow models, Sankarasubramanian et al. (2001) used the abcd model, Niemann and

Table 1. Summary of the elasticity notations used in this paper (X being precipitation P or potential evaporation E_P).

Notation	Definition	Formula
$\varepsilon_{Q/X}$	*Relative streamflow elasticity – percent* change of streamflow Q by *percent* change of climate variable X	$\frac{\Delta Q}{\overline{Q}} = \varepsilon_{Q/X} \frac{\Delta X}{\overline{X}}$
$e_{Q/X}$	*Absolute streamflow elasticity – mm* change of streamflow Q by *mm* change of climate variable X	$\Delta Q = e_{Q/X} \cdot \Delta X$

Table 2. Comparison of the theoretical and empirical elasticity assessment methods.

	Theoretical (model-based) elasticity assessment	Empirical (data-based) elasticity assessment
Co-variations of different climatic variables	The modeling approach distinguishes between the impact of different climatic variables (by keeping part of the forcing constant while modifying the other part).	Problem: the changes in observed climatic variables can be correlated (e.g., ΔP negatively correlated with ΔT when the driest years are also the warmest), which makes it more difficult to attribute streamflow changes to one or the other variable.
Data requirements	No need for long concomitant series of observed streamflow and climatic variables (only what is needed for model calibration).	Long concomitant series of observed streamflow and climatic variables are required.
Extrapolation capacity	Extrapolates to extreme climatic changes (i.e., to changes that have not been observed over historical records).	Can only deal with the changes that have been observed in the available historical record.

Eltahir (2005) used a purpose-built model and Chiew (2006) used the SIMHYD and AWBM models. The most widely used model in elasticity studies is the long-term water balance formula first proposed by Turc and Mezentsev (Mezentsev, 1955; Turc, 1954) (see Sect. 3.2). This formula (sometimes improperly confused with Budyko's formula) was used in elasticity studies by Dooge (1992), Arora (2002), Sankarasubramanian et al. (2001), Yang et al. (2008), Potter and Zhang (2009), Yang and Yang (2011), Donohue et al. (2011) and Yang et al. (2014), among others.

1.2.2 Empirical (data-based) studies

Only a few of the published elasticity studies are *empirical*. By *empirical*, we mean that they use measured data (for different sub-periods) to evaluate the climate elasticity of streamflow. To our knowledge, Sankarasubramanian et al. (2001) were the first to publish a method based on the median of annual flow anomalies to compute elasticity, later used by Chiew (2006). Potter et al. (2010) analyzed concomitant reductions of precipitation and streamflow in the Murray–Darling basin over three major historic droughts, and Potter et al. (2011) suggested computing elasticity as a multiple linear regression linking annual transformed streamflow values to annual precipitation and temperature anomalies.

1.2.3 Difference between theoretical (model-based) and empirical (data-based) elasticity assessments

To clarify the differences existing between theoretical and empirical elasticity computing approaches, we have listed the key characteristics of both methods in Table 2. The most important problem stems from the co-variation of potential evaporation (or temperature) and precipitation: Fu et al. (2007a) mentioned this issue and proposed to transform the "single parameter precipitation elasticity of streamflow index" into a "two parameter climate elasticity index" that would be a function of both precipitation and temperature, in order to account for both effects simultaneously. Recently, Chiew et al. (2013) underline that "because of the inverse correlation between rainfall and temperature, any effect from the residual temperature on streamflow is much less apparent than the direct effect of (the much more variable) rainfall". Note that the use of model simulations to compute streamflow elasticity circumvents this problem.

However, there remains what we consider to be a major disadvantage: since all hydrological models are a simplification of reality, using them to predict changes requires some type of initial validation on empirical (observed) data. Indeed, we have recently compared (see Fig. 9a in Coron et al., 2014) the ability of three models of increasing complexity to reproduce the variations in water balance equilibrium over 10-year long periods and shown that all three models tested had a tendency to underestimate observed changes.

In this paper, we will focus on identifying the most robust approach to computing empirical elasticity. Then we will compare the results obtained by this method with the theoretical elasticity of the Turc–Mezentsev water balance formula. This comparison will only aim at illustrating the difference between the two approaches, since there is no reason to consider one or the other to be the "true" reference.

1.3 Scope of the paper

In this paper, we test four alternative approaches to compute the empirical streamflow elasticity, which we compare over a large catchment set to the approach first suggested by Sankarasubramanian et al. (2001). In Sect. 2, we present the data set of 519 French catchments on which this study is based. Section 3 gives a short overview of the possible graphical representations of catchment elasticity and the methods used to quantify empirical elasticity. Section 4 presents a preliminary selection of the formulas, focusing on the distinction between univariate and bivariate methods. Then Sect. 5 presents a regional analysis of streamflow elasticity to precipitation and potential evaporation over France. Lastly, the conclusion identifies a few perspectives for further work.

2 Catchment data set

Figure 1 presents the 519 catchments analyzed for these studies.

Long series of continuous daily streamflow and precipitation were available over the 1976–2006 period. The data set encompasses a variety of climatic conditions (oceanic, Mediterranean, continental, mountainous). Precipitation data were provided by Météo France as a gridded product, based on a countrywide interpolation of rain gage data (SAFRAN product; see Le Moigne, 2002). As far as potential evaporation data are concerned, we used the Penman–Shuttleworth equation (Shuttleworth, 1993) because Donohue et al. (2010) suggested that it was the most appropriate form of *atmospheric evaporation demand* when considering a changing climate.

To illustrate the issues raised in this paper, we will use the catchment of the River Brèze at Meyrueis. This 36 km^2 catchment located in the south of France has a good-quality stream-gaging station and a long observation series.

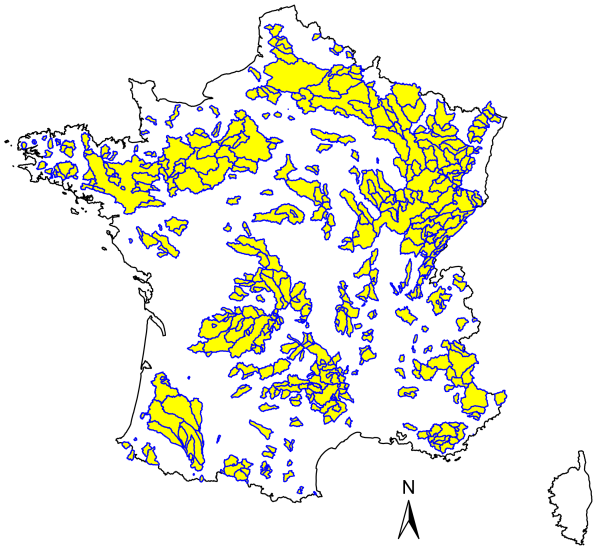

Figure 1. Locations of the 519 French catchments analyzed in this study.

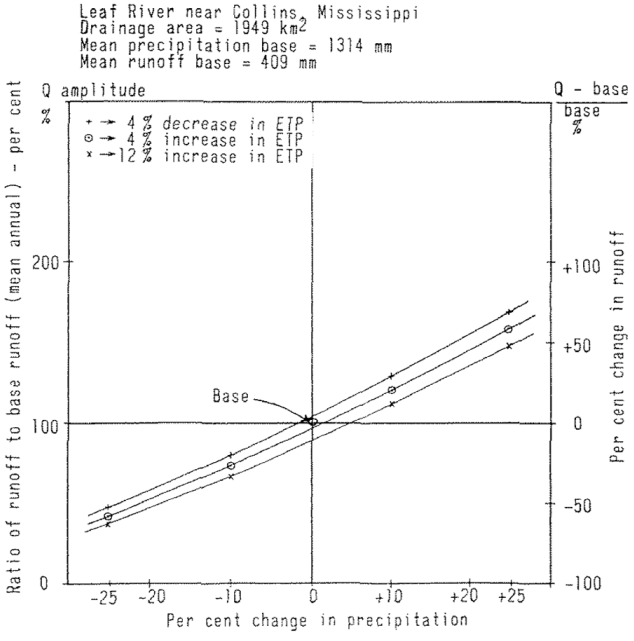

Figure 2. Yield change graph proposed by Nemec and Schaake (1982) to illustrate the hydrological elasticity analysis.

3 A review of methods to assess streamflow elasticity

3.1 Graphical assessment of elasticity

Nemec and Schaake (1982) introduced the classical sensitivity plots showing the changes in streamflow (or in some streamflow-based characteristics) as a function of percent change in precipitation (Fig. 2). Their approach consisted in assessing streamflow elasticity over the whole modeling period by gradually changing the model inputs individually. If the hydrological model behavior is free from thresholds or strong hysteresis effects, this method produces a set of parallel curves such as those shown in Fig. 2.

Wolock and McCabe (1999) used a similar graph (Fig. 3), but replaced the percent changes with the absolute changes (plotting $e_{Q/X}$ instead of $\varepsilon_{Q/X}$): in this paper, we will follow their example, but replace the model-based results with observations.

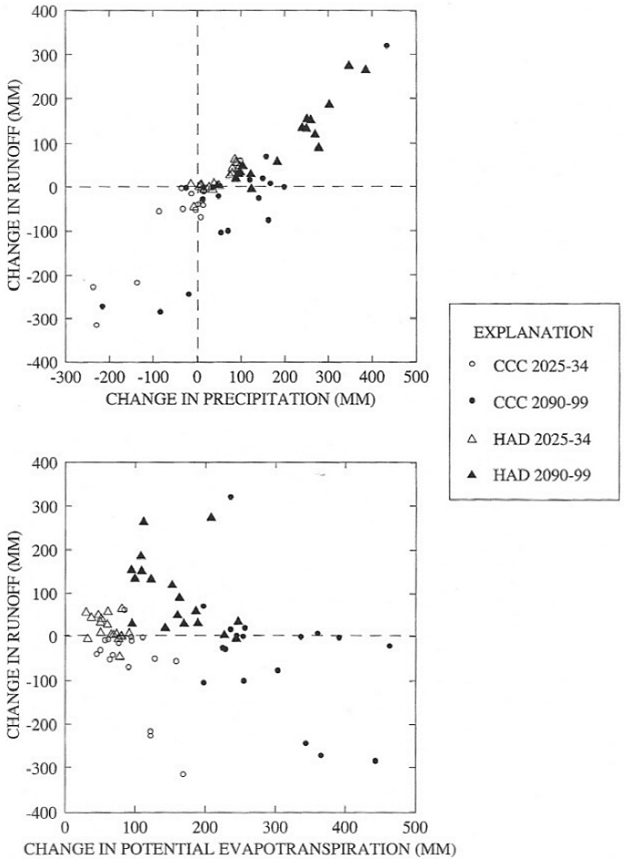

Figure 3. Elasticity graphs proposed by Wolock and McCabe (1999).

The graphs used herein describe *empirical elasticity*: they are based on hydrological data only and require a subsampling of long-term records, i.e., distinguishing a number of sub-periods. Therefore, a point is apparent for each of these sub-periods. Figure 4 presents an example in which ΔQ is plotted as a function of either ΔP or ΔE_P.

To represent the co-variations of ΔQ with both ΔP or ΔE_P simultaneously, we need either a three-dimensional graph or a graph based on isolines (see Fu et al., 2007b). Figure 4c presents an example using a color code. This graph is particularly useful because the values of ΔP and ΔE_P are often correlated (Chiew et al., 2013), which may make the two-dimensional representations misleading.

The graphical representation of empirical elasticity shown in Fig. 4 allows one to look at data without formulating an arbitrary modeling choice. The only convention lies in the duration of the sub-periods. Here, we chose a duration of 10 years in order to obtain contrasted yet representative periods. Figure 5 illustrates the changes induced by a change in this duration. It is reassuring to see that similar trends are observed for a wide range of period lengths. The relationship between the different variables does not remain absolutely identical, however, and there is clearly a trade-off between a longer duration, which ensures that the relationships are close to their long-term value, and a lower number of points, which reduces the confidence in the trend displayed by the plot.

3.2 Reference method for theoretical elasticity assessment: the Turc–Mezentsev formula

Most previous studies used a model-based definition of elasticity, and several of them used the Turc–Mezentsev formula (Mezentsev, 1955; Turc, 1954). The interested reader can refer to Lebecherel et al. (2013) for a historical review of this formula, which is given by

$$Q = \Psi(P, E_P) = P - \frac{P}{\left(1 + \left(\frac{P}{E_P}\right)^n\right)^{\frac{1}{n}}} = P - \left(P^{-n} + E_P^{-n}\right)^{\frac{-1}{n}}, \quad (3)$$

with Q the long-term mean average flow ($\mathrm{mm\,yr^{-1}}$), P the long-term mean average precipitation ($\mathrm{mm\,yr^{-1}}$), and E_P the long-term mean average potential evaporation ($\mathrm{mm\,yr^{-1}}$). n is the only free parameter of the formula. Here, we followed Le Moine et al. (2007) and used a fixed value: $n = 2.5$.

Partial derivatives of the Turc–Mezentsev formula are easily computed; they are given in Eqs. (4) and (5). They allow computing of the theoretical value of the precipitation and potential evaporation elasticity directly for each catchment.

$$\frac{\partial Q}{\partial E_P} = \Psi'_P(P, E_P) = -\left(1 + \left(\frac{E_P}{P}\right)^n\right)^{-\frac{n+1}{n}} \quad (4)$$

$$\frac{\partial Q}{\partial P} = \Psi'_{E_P}(P, E_P) = 1 - \left(1 + \left(\frac{P}{E_P}\right)^n\right)^{-\frac{n+1}{n}} \quad (5)$$

3.3 Alternative methods for empirical streamflow elasticity assessment

We will now focus on data-based methods assessing empirical elasticity. Long-term series of streamflow and catchment climate are required. Before introducing the methods compared in this paper, let us introduce the notation $\Delta X_i^{(M)} = X_i^{(M)} - X^{(\mathrm{LT})}$ denoting the departure (anomaly) of a variable X computed over a period of M years starting from year i vs. the long-term average $X^{(\mathrm{LT})}$ computed over the entire period.

Five methods will be compared in this paper, all listed in Table 3.

3.3.1 Nonparametric method

This method computes an annual time series of relative streamflow anomalies (i.e., differences with the long-term mean) and then uses the median of these values as an elastic-

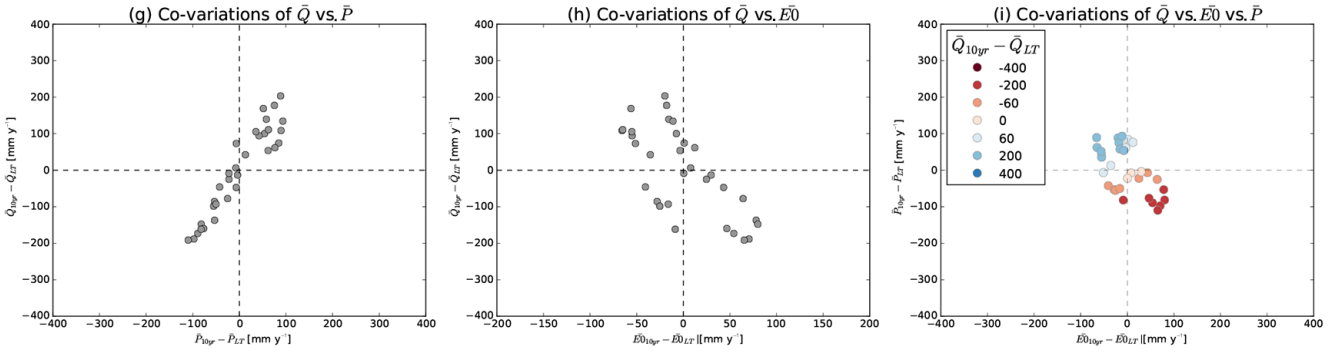

Figure 4. Streamflow elasticity graphs for an empirical (data-based) assessment for the Brèze catchment at Meyrueis (code: O3165010): **(a)** ΔQ vs. ΔP, **(b)** ΔQ vs. ΔE_P, and **(c)** ΔQ (color-coded) vs. ΔP and ΔE_P.

Table 3. Regression models used to assess empirical elasticity.

Notation	Definition	Inputs	Number of parameters
NP	Nonparametric regression	$\Delta P_i^{(M)}$ or $\Delta E_{P_i}^{(M)}$	0
OLS1	Ordinary least squares using a single climate input	$\Delta P_i^{(M)}$ or $\Delta E_{P_i}^{(M)}$	1
OLS2	Ordinary least squares using two climate inputs	$\Delta P_i^{(M)}$ and $\Delta E_{P_i}^{(M)}$	2
GLS1	Generalized least squares using a single climate input	$\Delta P_i^{(M)}$ or $\Delta E_{P_i}^{(M)}$	3
GLS2	Generalized least squares using two climate inputs	$\Delta P_i^{(M)}$ and $\Delta E_{P_i}^{(M)}$	4

ity estimator:

$$\begin{cases} e_{Q/P}^{(M)} = \text{median}\left(\dfrac{\Delta Q_i^{(M)}}{\Delta P_i^{(M)}}\right), \\ e_{Q/E_P}^{(M)} = \text{median}\left(\dfrac{\Delta Q_i^{(M)}}{\Delta E_{P_i}^{(M)}}\right). \end{cases} \quad (6)$$

This method is similar to the one advocated by Sankarasubramanian et al. (2001) except that they used it to compute the relative rather than the absolute elasticity (see Table 1). In addition, Sankarasubramanian et al. (2001) applied the method to yearly data only, whereas we used sub-periods ranging from 1 to 25 years in this study.

3.3.2 Regression methods quantifying precipitation and potential evaporation elasticities (OLS or GLS estimates) *independently*

These methods compute elasticity as either an ordinary least-square (OLS) or generalized least-square (GLS) solution (Johnston, 1972) of the regression models detailed in Table 4. See Appendix A for a quick description of the method used to perform the GLS regression.

3.3.3 Methods quantifying precipitation and potential evaporation elasticities (OLS or GLS estimates) *simultaneously*

These methods (OLS or GLS) quantify precipitation and potential evaporation elasticities *simultaneously* by looking for the GLS solution of a regression model with the same statistical assumptions as above (see Table 5).

The strength of the bivariate method obviously lies in the fact that it accounts for the cross-correlation of ΔP and ΔE_P values. The method used for inferring the parameter values and their significance was identical to the method described above.

Note that for the sake of consistency with the GLS models, the uncertainty in the OLS parameters was assessed with the bootstrap approach (Efron and Tibshirani, 1994).

4 Selection of the best method to compute empirical streamflow elasticity

4.1 Assessing the capacity of the five methods to compute the empirical elasticity of a synthetic data set

As a first step to compare the merits of the different regression models presented in the previous section, the elasticity estimation was conducted with synthetic streamflow data generated from the Turc–Mezentsev formula, where the parameter n was set at 2.5 (Le Moine et al., 2007) and input data from the 519 catchments described in Sect. 2. The advantage of using synthetic flow here is that we know the exact (i.e., analytical) solution for elasticity, and this will help identify the drawbacks of some of the methods compared.

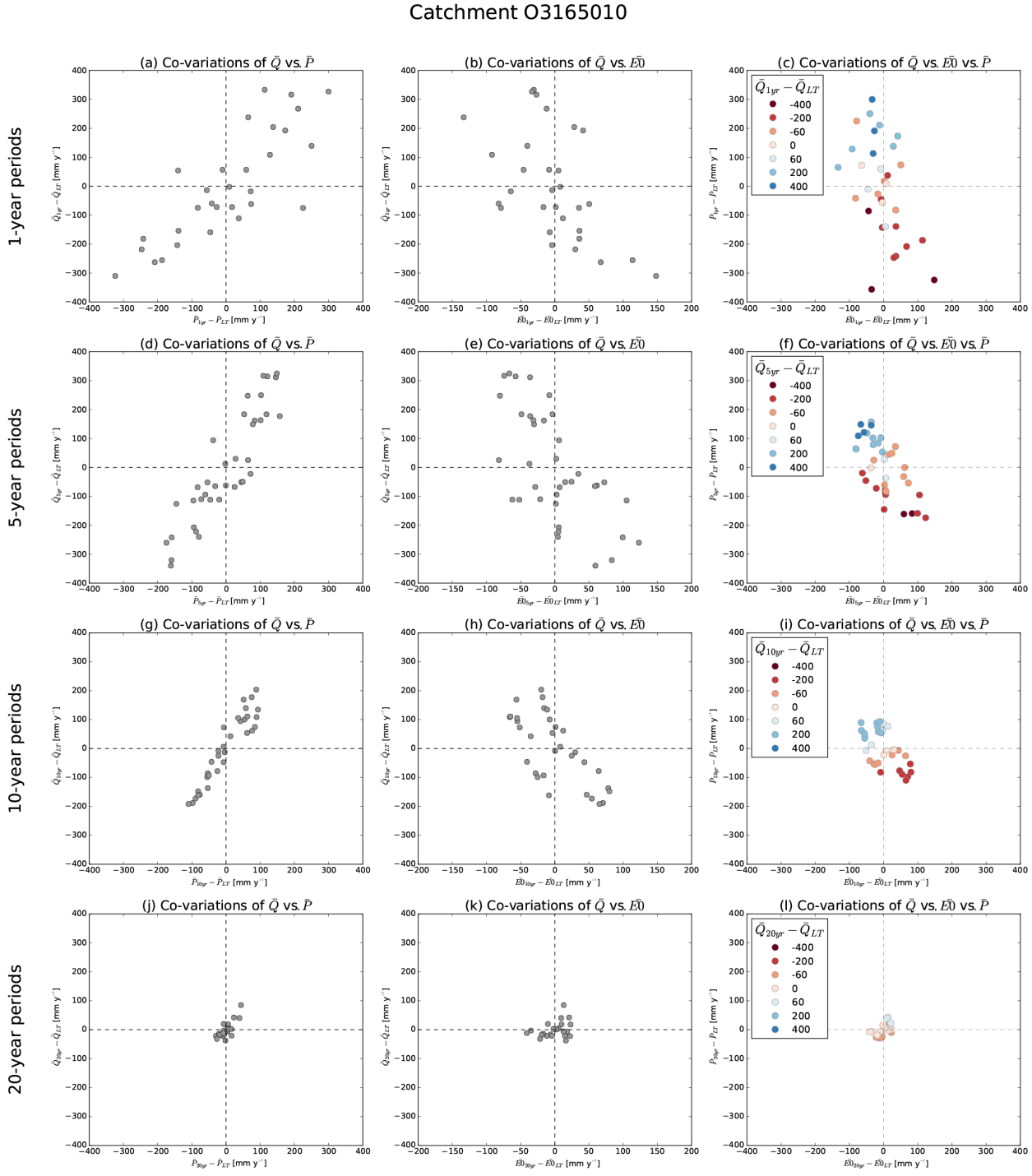

Figure 5. Impact of period length on the streamflow elasticity graphs for an empirical (data-based) assessment. The graphs present from left to right ΔQ vs. ΔP, ΔQ vs. ΔE_P, and ΔQ (in colors) vs. ΔP and ΔE_P. LT stands for long term (entire period).

For this test, the observed streamflow anomalies $\Delta Q_i^{(M)}$ were replaced by the estimates $\Delta \widetilde{Q}_i^{(M)} = \Psi\left(P_i^{(M)}, E_{P_i}^{(M)}\right) - \Psi\left(P^{(\mathrm{LT})}, E_{\mathrm{P}}^{(\mathrm{LT})}\right)$, where Ψ is given in Eq. (3). The empirical elasticity values were subsequently compared with the exact values $\Psi'_{\mathrm{P}}\left(P^{(\mathrm{LT})}, E_{\mathrm{P}}^{(\mathrm{LT})}\right)$ and $\Psi'_{E_{\mathrm{P}}}\left(P^{(\mathrm{LT})}, E_{\mathrm{P}}^{(\mathrm{LT})}\right)$ given in Eqs. (4) and (5), respectively. The performance of each regression model was judged according to the absolute bias B

Table 4. Univariate regression models for empirical elasticity assessment.

$\Delta Q_i^{(M)} = e_{Q/X}^{(M)} \cdot \Delta X_i^{(M)} + \omega_i$	
OLS	$\omega_i \sim N(0, \sigma)$
GLS	$\begin{cases} \omega_i = \alpha\omega_{i-1} + \delta_i \\ \delta_i \sim N(0, \sigma) \\ \omega_i \sim N(0, \sigma\sqrt{1-\alpha^2}) \end{cases}$

$\Delta Q_i^{(M)}$: streamflow anomaly over M years, considered as the explained variable
$\Delta X_i^{(M)}$: rainfall or potential evaporation anomaly for the same sub-period, considered as the explanatory variable
$e_{Q/X}^{(M)}$: streamflow elasticity (equal to the regression slope)
ω_i: regression residual
α: parameter of the first-order autoregressive process (AR1)
δ_i: innovation of the autoregressive process
σ: standard deviation
M: number of years over which the long-term streamflow, precipitation and evaporation average are computed

Table 5. Bivariate regression models for empirical elasticity assessment.

$\Delta Q_i^{(M)} = e_{Q/P}^{(M)} \cdot \Delta P_i^{(M)} + e_{Q/E_P}^{(M)} \cdot \Delta E_{P_i}^{(M)} + \omega_i$	
OLS	$\omega_i \sim N(0, \sigma)$
GLS	$\begin{cases} \omega_i = \alpha\omega_{i-1} + \delta_i \\ \delta_i \sim N(0, \sigma) \\ \omega_i \sim N(0, \sigma\sqrt{1-\alpha^2}) \end{cases}$

$\Delta Q_i^{(M)}$: streamflow anomaly over M years, considered as the explained variable
$\Delta X_i^{(M)}$: rainfall or potential evaporation anomaly for the same sub-period, considered as the explanatory variable
$e_{Q/X}^{(M)}$: streamflow elasticity (equal to the regression slope)
ω_i: regression residual
α: parameter of the first-order autoregressive process (AR1)
δ_i: innovation of the autoregressive process
σ: standard deviation
M: number of years over which the long-term streamflow, precipitation and evaporation average are computed

and the root mean square error (RMSE) R:

$$B_X^{(M)} = \left| \sum_{k=1}^{N} \left[e_{Q_i/X_i}^{(M)} - \Psi_x' \left(P_i^{(\mathrm{LT})}, E_{P_i}^{(\mathrm{LT})} \right) \right] \right|, \quad (7)$$

$$R_X^{(M)} = \sqrt{\sum_{i=1}^{N} \left[e_{Q_i/X_i}^{(M)} - \Psi_x' \left(P_i^{(\mathrm{LT})}, E_{P_i}^{(\mathrm{LT})} \right) \right]^2}, \quad (8)$$

where X is the climate variable (P or E_P), $e_{Q_i/X_i}^{(M)}$ is the corresponding empirical elasticity value computed for catchment i using sub-periods of M years, and $N = 519$ is the number of catchments.

The performance of the five alternative methods is presented in Fig. 6, which shows the absolute bias and the root mean square error in the elasticity for precipitation and potential evaporation, respectively.

The four plots in Fig. 6 clearly indicate the superiority of the two bivariate models (OLS-2 and GLS-2) over the three univariate models (NP, OLS-1 and GLS-1), with bias and RMSE in both types of elasticity that are lower by several orders of magnitude. This first result suggests that the estimation of empirical elasticity is greatly improved when conducted simultaneously on rainfall and potential evaporation.

Figure 6 also shows that the duration of the sub-periods can slightly affect the performance of the regression model. The largest impact can be seen in the bias in the elasticity to potential evaporation (Fig. 6a), where the optimal duration of 20 years provides a better performance compared to the other durations. The 20-year duration seems to be the best choice for both types of elasticity, for all regression models, and both bias and RMSE.

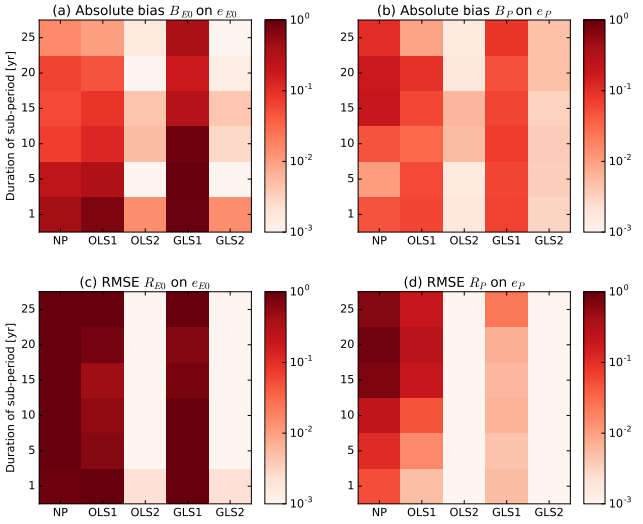

Figure 6. Performances of the five models proposed to compute empirical elasticity, tested on synthetic data generated with the Turc–Mezentsev model.

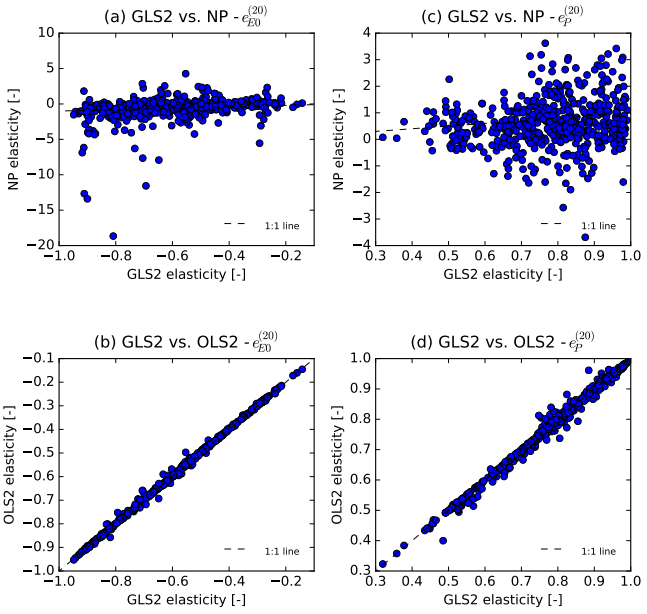

Figure 7. Comparison of elasticity estimates obtained with the GLS2, OLS2 and NP methods using synthetic flow data and 20-year sub-periods.

This study based on synthetic data shows the clear superiority of the methods based on bivariate regressions (OLS2 and GLS2): the nonparametric (NP) method and the univariate regressions (OLS1 and GLS1) are clearly unable to compute streamflow elasticity robustly. Because the NP method is the reference method (suggested by Sankarasubramanian et al., 2001), Fig. 7a and c compare the empirical elasticity values given by the NP method and the GLS2 method: the differences are very large. On the other hand, Fig. 7b and d show that there is little difference between the estimates given by OLS2 and GLS2. However, for statistical reasons (presented in Appendix B), we consider that the GLS method should be preferred.

Having decided on the best method to compute empirical elasticity, we can now compare model elasticities with the GLS estimates based on measured streamflow.

4.2 Coherence of data-based and model-based elasticity estimates

We now wish to compare the *empirical* elasticity computed with the GLS2 method (the recommended one) with the *theoretical* elasticity derived analytically from the Turc–Mezentsev formula (see Eq. 3). While in the previous test we used synthetic data, we now use the actual (measured) streamflow. This means that contrary to the preceding test, we do not have any "reference": since neither the data-based nor the model-based elasticity can be considered "true", we can only assess the coherence between the two computations.

The scatterplots illustrated in Fig. 8 compare the elasticity values obtained by the multivariate regression (GLS2) method and the model-based approach: we can see that the link between the two measurements on a catchment-by-catchment basis is extremely weak for precipitation, and even more so for potential evaporation.

The fact that empirical and theoretical elasticities differ is in itself noteworthy and would require further analysis. At this point, we cannot draw any further conclusion from this comparison: as widely used as it is, the Turc–Mezentsev relationship remains a theoretical model and cannot be considered superior to the data-based elasticity assessment.

5 Results: regional elasticity analysis over France

Henceforth, we only consider the empirical elasticity estimates given by the GLS2 method. Figure 9 illustrates the results: each of the 519 gauging stations of the data set is shown, but the points for which the elasticity coefficient is not significantly different from zero are indicated with a cross only. For the other points, the color code gives the elasticity value.

From the maps, it is difficult to identify physical reasons for the spatial variations in elasticity values. The Massif central highlands seem to show a slightly higher occurrence of high-intensity elasticities, both to P and E_P, and the Paris Basin lowlands a slightly lower occurrence. This tendency could perhaps be related to the absence/presence of large groundwater aquifers, but more detailed comparative studies are needed to draw a firm conclusion.

A few outliers appear, which is common when using a large data set: five catchments shows a negative elasticity to precipitation and 48 catchments show a positive elasticity to potential evaporation (see detailed results in Appendix C and

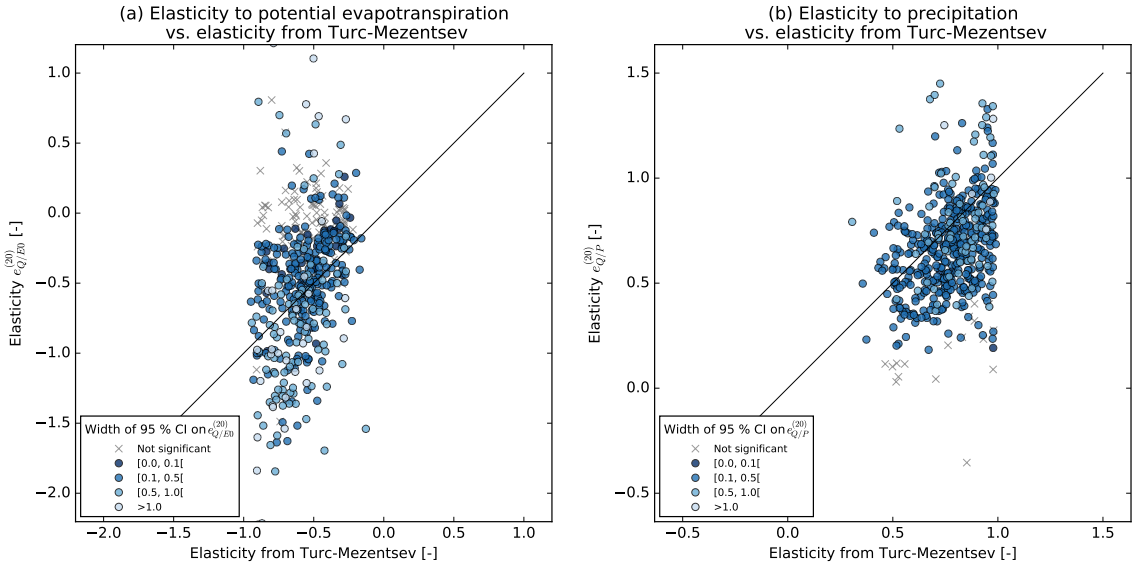

Figure 8. Comparison of the data-based and model-based elasticities; streamflow elasticity to potential evaporation **(a)** and precipitation **(b)**. The points are colored according to the width of the 95 % bootstrap confidence intervals on the empirical elasticity estimate.

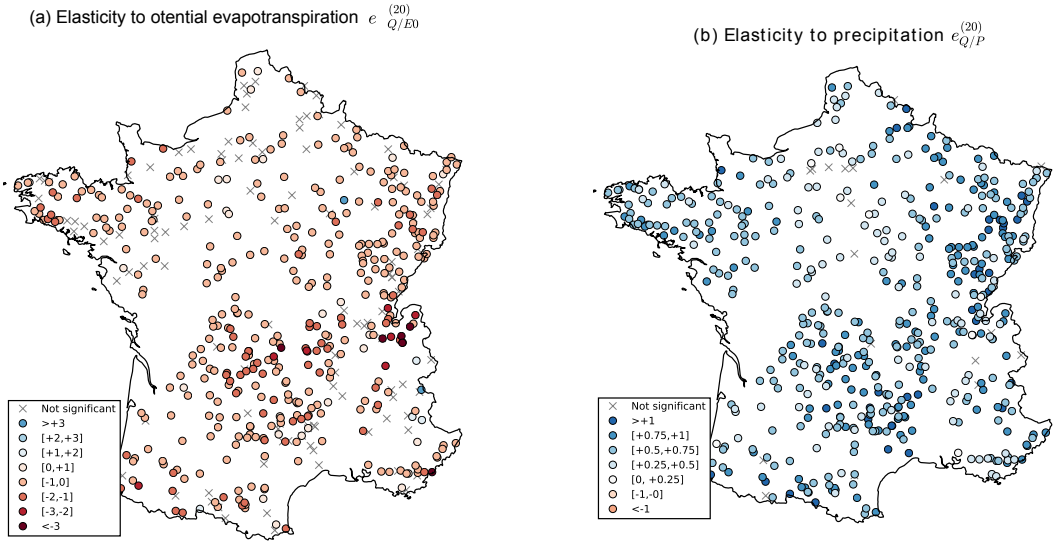

Figure 9. Regional analysis of **(a)** streamflow elasticity to precipitation and **(b)** streamflow elasticity to potential evaporation. Elasticity values were obtained by the GLS2 regression method using 20-year sub-periods. Each dot represents a catchment outlet; the color represents the elasticity value. Those catchments where the linear correlation was found to be nonsignificant are indicated with a cross.

the corresponding plots in Supplement). In almost all cases, the linear regression was not significant We checked each of the plots individually and verified that this was in fact due to a very limited span of streamflow anomaly ΔQ, which made the regression rather meaningless.

To conclude this countrywide analysis of elasticity, we tested a possible relation between catchment size and elasticity values. Figure 10 speaks for itself: over the range of catchment areas covered by this study, no trend could be identified with catchment area.

6 Conclusion

6.1 Synthesis

In this paper, we identified an improved method to assess the empirical elasticity of streamflow to precipitation and potential evaporation. This method (GLS2), which uses long-term hydrometeorological records, was tested on a set of 519 French catchments.

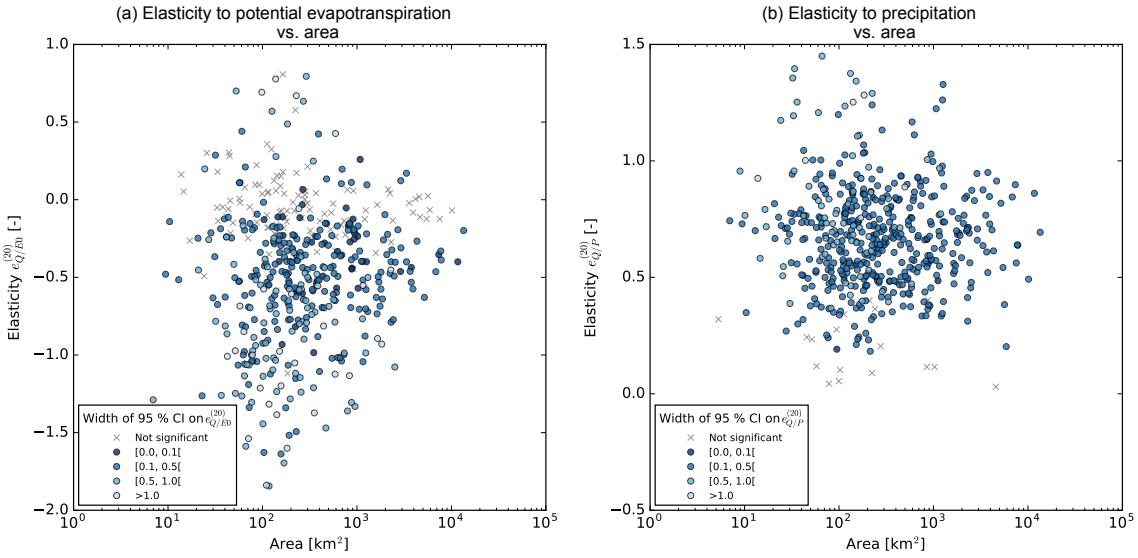

Figure 10. Elasticity values vs. catchment area: **(a)** streamflow elasticity to potential evaporation and **(b)** streamflow elasticity to precipitation. Elasticity values were obtained by the GLS2 regression method with sub-periods of 10 years. The points are colored according to the width of the 95 % bootstrap confidence intervals on the GLS2 elasticity estimate.

We started with a synthetic data set and compared this improved method with the reference nonparametric method and with several univariate and bivariate alternatives: we obtained results with a much lower bias and RMSE, this difference being clearly due to the fact that the improved method was able to account for the covariation of precipitation and potential evaporation anomalies.

We then compared the improved empirical elasticity estimate with the theoretical estimates derived analytically from the Turc–Mezentsev formula. Empirical and theoretical estimates correlated weakly: the link between the two measurements on a catchment-by-catchment basis is weak for precipitation, and very weak for potential evaporation.

6.2 Limits and perspectives

As a simple method characterizing the sensitivity of streamflow to climatic changes, the identification of empirical elasticity seems promising. Indeed, the empirical elasticity assessment advocated in this paper can provide an estimate of the impact of climate change on hydrology that is *almost* model-free (except for the assumption of linearity, of course) and allows digging into *past* observations to predict the impact of *future* changes. Another perspective can also be seen for studies involving hydrological models for climate change assessment: empirical elasticity could provide a very useful benchmark against which to test the predictions of complex hydrological models (see, e.g., how the extrapolation capacity of several hydrological models was assessed in Coron et al., 2014).

Naturally, the elasticity assessment has its limits: there is no guarantee of its ability to extrapolate to the most extreme climatic changes (i.e., to changes that are far from those observed over historical records). The formula chosen to compute potential evaporation is also a concern. In this paper, we used the Penman–Shuttleworth equation (Shuttleworth, 1993). We also repeated this study with the Oudin et al. (2005) formula (a formula widely used in France) and the Penman–Monteith equation (Allen et al., 1998), which did not yield significant differences. This result was expected because the catchments considered here are energy-limited with few cases where actual evaporation reaches its potential value. However, for other climates (i.e., drier environments), additional work would be required to further test the sensitivity of streamflow elasticity to the potential evaporation formula.

7 Data availability

This paper is based on climatic data provided by Météo France, which does not allow their redistribution, and on streamflow data which are freely accessible through the Banque Hydro portal http://www.hydro.eaufrance.fr/. Long-term catchment-aggregated values are presented in Appendix C.

Appendix A: GLS regression

The parameters of the GLS regression were inferred by maximizing the log-likelihood function associated with this model:

$$L\left(\left\{\Delta Q_i^{(M)}\right\},\left\{\Delta X_i^{(M)}\right\}|e_{Q/X}^{(M)},\sigma,\alpha\right)= -\frac{k}{2}\log(2\pi)-k\log(\sigma)-\frac{1}{2}\log(1-\alpha^2) -\frac{1}{2\sigma^2}\left(\left(1-\alpha^2\right)\omega_1^2+\sum_{i=2}^{k}(\omega_i-\alpha\omega_{i-1})^2\right), \quad \text{(A1)}$$

where k is the number of sub-periods. The optimization was performed with the Nelder–Mead algorithm (Nelder and Mead, 1965) using the ordinary least-square solution (OLS) as a starting point (i.e., the solution of the same regression model with $\alpha = 0$). The validity of the model assumptions was checked (see Appendix B) by computing the Shapiro–Wilks test (with an expected p value greater than 0.05) and Durbin–Watson statistic (with an expected value greater than 1) from the series of innovations $\hat{\delta}_i$:

$$\hat{\delta}_i = \hat{\omega}_i - \alpha\hat{\omega}_{i-1} \text{ if } i > 1 \text{ and } \hat{\delta}_1 = \hat{\omega}_1, \quad \text{(A2)}$$

$$\hat{\omega}_i = \Delta Q_i^{(M)} - e_{Q/X}^{(M)}\Delta X_i^{(M)}. \quad \text{(A3)}$$

Unlike the OLS solution, the distribution of the elasticity values obtained with this approach does not have a closed form. As a result, the significance of the regression's coefficients was assessed with a bootstrap approach as follows.

a. The GLS model was fit with the maximum likelihood approach first. This allowed computing of the series of innovations δ_i.

b. The innovations $\{\delta_i\}_{i=2,\ldots,n}$ were resampled with replacement to form a new series of bootstrapped innovations $\left\{\delta_i^*\right\}_{i=2,\ldots,n}$. The first innovation δ_1^* of this series was set to ω_1.

c. The bootstrapped innovations were used to generate a new series of bootstrapped observations $\Delta Q_i^{(M)*} = e_{Q/X}^{(M)}\Delta X_i + \sum_{i=1}^{n}\delta_i^*\alpha^i$.

d. Finally the GLS model was fit with the maximum likelihood approach using the bootstrapped observations, leading to new values of the GLS parameters.

Steps (c) and (d) were repeated 1000 times and the 2.5 and 97.5% percentiles of the GLS parameters were derived from the empirical distribution formed with the 1000 parameter samples. A parameter was considered significantly different from zero if both the 2.5 and 97.5% percentiles were either strictly positive or negative.

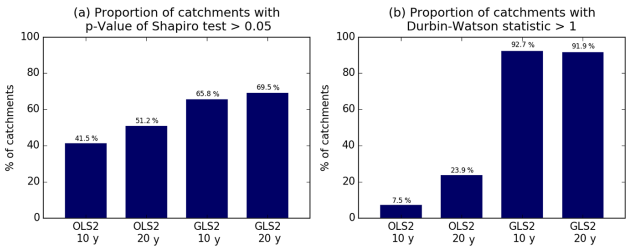

Figure B1. Proportion of catchments having a positive outcome for **(a)** the Shapiro–Wilks normality test and **(b)** the Durbin–Watson test on autocorrelation of innovations.

Appendix B: Validity of statistical assumptions underlying the regression models

This section reviews the validity of the statistical assumptions underlying the OLS2 and GLS2 regression models described in Sect. 3.3.

- Figure B1a shows that the GLS2 model has the highest proportion of catchments where the normality assumption cannot be rejected based on the Shapiro–Wilks test. However, the difference with the other models remains limited, with this proportion varying from 41.2% for OLS2 with 10-year sub-periods to 69.5% for GLS2 with 20-year sub-periods. Overall, a significant proportion of catchments still fail the test, whatever regression model is considered, which suggests that additional assumptions could be explored for the distribution of the innovations.

- Figure B1b reveals that a high level of autocorrelation is present in the innovations of the OLS2 model, with 7.5% (with 10-year sub-periods) and 23.9% (with 20-year sub-periods) of the catchments reaching a satisfactory Durbin–Watson statistic value only. This was an expected result. Logically, this proportion is much higher for the GLS2 models, reaching 92.7% for 10-year sub-periods and 91.9% for 20-year sub-periods. Here also, a small proportion of the catchments fails the test, even with regression models taking autocorrelation into account. This result suggests that the regression model could be extended to include a higher-order autoregressive component.

Overall, the results illustrated in Fig. B1 indicate that the GLS2 model is the most satisfactory regression model from a statistical point of view. The difference introduced by the length of the averaging period (10 or 20 years) is very limited.

Appendix C: Complete elasticity figures for our dataset

Table C1. Main characteristics of the catchment data set. Note: all long-term values have been computed over the 1986–2006 time period.

Catchment code	e_{Q/E_P}	$e_{Q/P}$	Altitude of the outlet (m a.s.l.)	Area (km^2)	X outlet (DD)	Y outlet (DD)	Long-term precipitation P (mm yr^{-1})	Long-term potential evaporation E (mm yr^{-1})	Long-term streamflow Q (mm yr^{-1})	River name
A1050310	−0.74	0.58	282	238	7.2439	47.6252	983	666	312	L'Ill à Altkirch
A1080330	−0.58	0.54	242	668	7.3058	47.7172	962	671	298	L'Ill à Didenheim
A1152010	−0.42	0.48	256	288	7.2481	47.6710	964	672	316	La Largue à Illfurth
A2023030	−0.58	0.54	432	44	7.1103	48.0515	1563	587	994	La Petite Fecht à Stosswihr
A2073010	−0.38	0.86	303	31	7.3016	48.1995	1390	633	362	Le Strengbach à Ribeauvillé
A2122010	0.05	0.68	326	118	7.2140	48.1563	1344	618	654	La Weiss à Kaysersberg (Fréland-Gare)
A2332110	−0.52	0.69	262	107	7.2921	48.2701	1372	627	518	La Lièpvrette à Lièpvre
A2512010	−1.25	0.91	221	42	7.4221	48.3862	1261	618	585	L'Andlau à Andlau
A2612010	−0.60	0.71	161	57	7.5111	48.4517	1036	659	290	L'Ehn à Niedernai
A2732010	−1.31	1.08	267	224	7.2751	48.5051	1302	604	825	La Bruche à Russ (Wisches)
A2842010	0.04	1.01	169	167	7.4892	48.5725	821	675	269	La Mossig à Soultz-les-Bains
A3151010	−0.22	0.66	146	280	7.7299	48.8258	813	682	277	La Moder à Schweighouse-sur-Moder (amont)
A3301010	−0.37	0.52	144	622	7.7418	48.8225	845	676	272	La Moder à Schweighouse-sur-Moder (aval)
A3422010	−0.57	0.45	196	184	7.3331	48.7287	1089	652	369	La Zorn à Saverne (Schinderthal)
A3472010	0.23	0.80	147	684	7.6335	48.7499	849	677	286	La Zorn à Waltenheim-sur-Zorn
A3712010	−0.84	0.41	176	192	7.7575	48.9587	902	665	283	La Sauer à Goersdorf (Liebfrauenthal)
A3832010	−0.59	0.78	124	204	8.0483	48.9037	833	687	251	Le Seltzbach à Niederroedern
A3902010	−0.64	0.38	173	275	7.9019	49.0422	909	662	280	La Lauter à Wissembourg (Weiler)
A4050620	−0.98	1.73	439	152	6.6861	47.9096	1650	600	1402	La Moselle à Rupt-sur-Moselle
A4142010	−0.58	1.11	407	184	6.7133	47.9959	1687	577	1460	La Moselotte à Vagney (Zainvillers)
A4173010	−0.61	0.98	455	65	6.6899	48.0526	1665	594	1205	La Cleurie à Cleurie
A4200630	−0.71	0.99	372	627	6.6103	48.0655	1651	598	1207	La Moselle à Saint-Nabord (Noirgueux)
A4250640	−0.88	0.90	325	1218	6.4529	48.1656	1553	609	983	La Moselle à Épinal
A5261010	−0.72	0.74	265	383	6.1373	48.3050	1016	649	381	Le Madon à Mirecourt
A5431010	−0.31	0.77	225	948	6.1317	48.5446	945	654	364	Le Madon à Pulligny
A5730610	−0.38	0.88	200	3346	5.8976	48.6698	1171	641	609	La Moselle à Toul
A6051020	−0.51	0.59	339	371	6.9561	48.2847	1588	611	667	La Meurthe à Saint-Dié
A6151030	−0.70	0.51	282	727	6.8447	48.4025	1558	623	614	La Meurthe à Raon-l'Étape
A6571110	−0.18	0.81	220	560	6.4868	48.5948	970	657	384	La Vezouze à Lunéville
A6731220	−0.45	0.75	234	498	6.5243	48.4872	1166	655	366	La Mortagne à Gerbéviller
A6761010	−0.52	0.96	211	2294	6.3839	48.5632	1207	646	482	La Meurthe à Damelevières
A6953010	−0.18	1.32	198	85	6.1982	48.7467	825	675	283	L'Amézule à Lay-Saint-Christophe
A7010610	−0.54	0.90	184	6835	6.1237	48.7896	1124	649	529	La Moselle à Custines
A7122010	−0.16	0.73	187	228	6.0434	48.8659	829	672	204	L'Esch à Jezainville
A7642010	−0.41	0.41	200	150	6.5060	48.8173	882	671	259	La Petite Seille à Château-Salins
A7821010	−0.22	0.71	180	928	6.2278	48.8880	842	674	267	La Seille à Nomeny
A7881010	−0.16	0.67	164	1274	6.1877	49.1007	825	674	246	La Seille à Metz
A8431010	0.06	1.17	167	1241	6.0715	49.2564	882	657	304	L'Orne à Rosselange
A9942010	−0.39	0.72	191	1150	6.5397	49.3012	835	659	279	La Nied à Bouzonville
B0220010	−0.18	0.65	300	368	5.6139	48.2406	960	658	365	La Meuse à Goncourt
B1092010	−1.02	0.40	291	401	5.7104	48.3171	1002	644	346	Le Mouzon à Circourt-sur-Mouzon (Villars)
B2220010	−0.46	0.75	216	2543	5.5310	48.8709	978	649	384	La Meuse à Saint-Mihiel
B3150020	−0.59	0.84	162	3915	5.1780	49.4939	975	650	397	La Meuse à Stenay
B4631010	−0.26	0.74	159	1978	5.1592	49.6292	929	642	412	La Chiers à Carignan
B5322010	0.00	0.77	153	125	4.7142	49.7277	1021	635	584	La Vence à la Francheville
D0206010	0.06	0.79	133	115	3.9971	50.2613	906	635	397	La Solre à Ferrière-la-Grande
E1766010	−0.15	0.26	37	88	3.5325	50.3304	769	649	220	La Rhonelle à Aulnoy-lez-Valenciennes
E1827020	−0.31	0.99	15	241	3.6376	50.4379	770	649	267	L'Hogneau à Thivencelle
E3346010	−0.35	0.45	26	132	3.1820	50.5783	762	665	218	La Marque à Bouvines
E3511210	−1.45	0.81	83	87	2.1734	50.5219	1068	623	409	La Lys à Lugy
E4035710	0.12	0.79	19	392	2.2448	50.7085	1026	620	461	L'Aa à Wizernes
E5300210	−0.90	0.73	26	103	1.7677	50.6812	1054	632	574	La Liane à Wirwignes
E5400310	−0.08	0.44	6	917	1.8308	50.4483	1002	629	435	La Canche à Brimeux
E5406510	−0.08	0.55	24	345	2.0378	50.3799	997	627	428	La Ternoise à Hesdin
E5505720	0.06	0.36	12	792	1.9177	50.3050	904	634	332	L'Authie à Dompierre-sur-Authie
E6470910	0.08	0.34	4	5643	1.8793	50.0625	744	649	205	La Somme à Abbeville (Epagne-Epagnette)

Table C2. Continued.

Catchment code	e_{Q/E_p}	$e_{Q/P}$	Altitude of the outlet (m a.s.l.)	Area (km^2)	X outlet (DD)	Y outlet (DD)	Long-term precipitation P ($mm\,yr^{-1}$)	Long-term potential evaporation E ($mm\,yr^{-1}$)	Long-term streamflow Q ($mm\,yr^{-1}$)	River name
G1003010	−0.58	0.69	15	255	1.3381	50.0001	963	635	337	L'Yères à Touffreville-sur-Eu
H0100010	−0.57	0.67	249	373	4.5700	47.7649	949	669	384	La Seine à Nod-sur-Seine
H0100020	−1.07	0.87	180	686	4.4806	47.9960	919	678	486	La Seine à Plaines-Saint-Lange
H0400010	−0.24	0.66	149	2340	4.3767	48.1166	906	678	340	La Seine à Bar-sur-Seine
H0400020	−0.13	0.60	139	2392	4.3107	48.1474	904	678	208	La Seine à Courtenot
H0503010	−0.09	0.64	109	249	4.1097	48.2459	795	690	184	L'Hozain à Buchères (Courgerennes)
H1051020	−0.29	0.66	185	690	4.7959	48.1454	948	668	336	L'Aube (partielle) à Longchamp-sur-Aujon (Outre Aube)
H1333010	1.62	1.87	137	22	4.7353	48.3788	877	685	1447	La Laine à Soulaines-Dhuys
H1513210	−0.38	0.72	86	171	4.0628	48.5380	713	687	131	La Barbuise à Pouan-les-Vallées
H1603010	−0.21	0.46	78	366	3.9053	48.6139	730	680	133	La Superbe à Saint-Saturnin
H1932020	0.04	0.43	63	281	3.2347	48.4878	749	684	187	La Voulzie à Jutigny
H2062010	−0.61	0.29	161	264	3.4936	47.4144	891	702	238	Le Beuvron à Ouagne (Champmoreau)
H2073110	−1.00	0.40	170	87	3.4078	47.4305	912	696	318	Le Sauzay à Corvol-l'Orgueilleux
H2083110	−0.32	0.52	150	192	3.5090	47.5096	824	693	244	La Druyes à Surgy
H2322010	−0.49	0.47	312	267	4.2917	47.4181	949	676	262	Le Serein à Bierre-lès-Semur
H2342010	−0.35	0.51	129	1116	3.8002	47.8176	873	691	224	Le Serein à Chablis
H2412010	−0.20	0.58	205	478	4.2627	47.6075	902	678	217	L'Armançon à Quincy-le-Vicomte
H2513110	−0.43	0.75	88	133	3.3552	47.9392	752	711	187	Le Tholon à Champvallon
H3102010	−0.39	0.49	187	152	3.2926	47.7329	825	686	192	L'Ouanne à Toucy
H3122010	−0.46	0.46	133	559	3.0908	47.8855	814	691	195	L'Ouanne à Charny
H3201010	−0.38	0.64	78	2302	2.7322	48.0356	747	701	156	Le Loing à Châlette-sur-Loing
H3613010	−0.14	0.22	86	162	2.8603	48.2455	742	703	92	Le Lunain à Paley
H3623010	−0.15	0.23	105	104	3.0234	48.2564	778	701	107	L'Orvanne à Blennes
H4022020	−0.20	0.19	56	851	2.3475	48.4643	660	705	135	L'Essonne à Guigneville-sur-Essonne (La Mothe)
H4223110	−0.16	0.43	80	152	2.0333	48.5700	675	683	134	La Remarde à Saint-Cyr-sous-Dourdan
H4243010	−0.18	0.55	54	231	2.2335	48.7006	675	682	187	L'Yvette à Villebon-sur-Yvette
H5062010	−0.14	0.76	206	618	5.1655	48.3440	1027	659	486	Le Rognon à Doulaincourt-Saucourt
H5142610	−0.39	0.79	170	114	5.0558	48.8836	1072	653	438	La Chée à Villotte-devant-Louppy (Villote devant Loupy)
H5172010	−0.23	0.78	95	2109	4.6271	48.7460	1033	657	411	La Saulx à Vitry-en-Perthois
H5732010	−0.06	0.84	62	769	3.0131	48.8174	763	678	232	Le Grand Morin à Pommeuse
H6102010	−0.63	0.73	222	283	5.2090	48.9645	1089	646	413	L'Aire à Beausite (Amblaincourt)
H6122010	−0.56	0.97	154	629	5.0342	49.2275	1055	649	464	L'Aire à Varennes-en-Argonne
H6162010	−0.40	0.92	117	957	4.9036	49.3338	1032	651	445	L'Aire à Chevières
H6201010	−0.44	0.78	100	2242	4.7827	49.3075	954	660	341	L'Aisne à Mouron
H6221010	−0.48	0.84	77	2888	4.5377	49.4920	942	659	342	L'Aisne à Givry
H6313020	−0.19	0.27	59	810	4.0238	49.3835	755	668	161	La Suippe à Orainville
H6423010	−0.05	0.58	58	300	3.6736	49.3061	712	663	166	L'Ardres à Fismes
H6531011	−0.23	0.57	33	7810	2.9521	49.4108	832	664	287	L'Aisne à Trosly-Breuil (Hérant)
H7021010	−0.09	0.59	160	320	4.0709	49.9227	1034	623	547	L'Oise à Hirson
H7033010	−0.95	0.90	140	256	4.0199	49.8956	990	634	463	Le Thon à Origny-en-Thiérache
H7041010	−0.27	0.85	101	860	3.7003	49.8996	987	633	467	L'Oise à Monceau-sur-Oise
H7061010	−0.35	0.80	70	1193	3.4821	49.8399	949	635	330	L'Oise à Origny-Sainte-Benoite
H7162010	−0.17	0.85	51	1637	3.4843	49.6926	848	654	291	La Serre à Pont à Bucy
H7401010	−0.21	0.57	35	4320	2.9939	49.5597	843	652	256	L'Oise à Sempigny
H7423710	−0.24	0.36	33	280	2.8464	49.4418	696	663	140	L'Aronde à Clairoix
H7611012	−0.14	0.60	26	13 484	2.6211	49.3105	824	661	264	L'Oise à Pont-Sainte-Maxence (Sarron)
H7713010	−0.52	0.31	89	214	1.9986	49.5287	843	633	238	Le Petit Thérain à Saint-Omer-en-Chaussée
H7742010	−0.82	0.68	61	755	2.0998	49.4220	843	639	238	Le Thérain à Beauvais
H7742020	−0.25	0.42	33	1210	2.3779	49.2623	799	647	223	Le Thérain à Maysel
H7833520	0.05	0.09	32	58	2.3997	49.1365	707	690	120	L'Ysieux à Viarmes (Giez)
H7853010	−0.23	0.22	37	102	2.1710	49.1266	713	671	167	Le Sausseron à Nesles-la-Vallée
H8012010	−0.66	0.63	87	247	1.7288	49.4728	971	636	248	L'Epte à Gournay-en-Bray
H8043310	0.02	−0.01	40	99	1.6901	49.1510	732	664	149	L'Aubette de Magny à Ambleville
H8212010	−0.45	0.53	53	377	1.3833	49.4454	973	636	338	L'Andelle à Vascoeuil
H9202010	0.15	0.44	119	477	1.1049	48.7617	738	666	175	L'Avre à Acon
H9222010	0.12	0.35	78	872	1.3467	48.7748	701	666	133	L'Avre à Muzy
H9331010	0.08	0.28	24	4561	1.2087	49.1151	661	674	128	L'Eure à Cailly-sur-Eure
H9402030	−0.15	0.26	47	1029	1.1507	49.0804	690	666	115	L'Iton à Normanville
H9501010	−0.13	0.11	13	5891	1.1775	49.2244	667	672	134	L'Eure à Louviers

Table C3. Continued.

Catchment code	e_{Q/E_p}	$e_{Q/P}$	Altitude of the outlet (m a.s.l.)	Area (km^2)	X outlet (DD)	Y outlet (DD)	Long-term precipitation P ($mm\,yr^{-1}$)	Long-term potential evaporation E ($mm\,yr^{-1}$)	Long-term streamflow Q ($mm\,yr^{-1}$)	River name
I0113010	−0.17	0.51	166	82	0.4851	48.9452	819	642	248	Le Guiel à Montreuil-l'Argillé
I0122010	−0.20	0.47	127	251	0.5684	49.0237	819	641	272	La Charentonne à Ferrières-Saint-Hilaire
I1203010	−0.38	0.46	32	173	0.2855	49.2978	813	659	323	La Calonne aux Authieux-sur-Calonne
I2001010	−0.41	0.57	90	88	0.0745	48.8149	747	663	156	La Dives à Saint-Lambert-sur-Dive
I2021010	−0.37	0.37	53	283	−0.0778	48.8982	732	663	164	La Dives à Beaumais
I2213610	−0.07	0.52	6	57	−0.0688	49.2346	772	666	251	L'Ancre à Cricqueville-en-Auge
I3131010	−0.23	0.64	106	1019	−0.3029	48.7927	821	659	232	L'Orne à Rabodanges
I4032010	−0.76	0.63	8	256	−0.5305	49.2910	877	662	293	La Seulles à Tierceville
I5053010	1.15	0.24	76	116	−0.8883	48.9474	941	643	421	La Souleuvre à Carville
I7222020	0.47	1.62	18	141	−1.4438	49.0363	1032	659	542	La Soulles à Saint-Pierre-de-Coutances
I7913610	−0.27	0.70	9	73	−1.5317	48.7843	1014	669	398	Le Thar à Jullouville
J0014010	−1.09	0.44	111	65	−1.1988	48.3744	878	675	312	Le Nançon à Lécousse (Pont aux Anes)
J0144010	−0.76	0.54	58	82	−1.4364	48.4292	870	680	290	La Loysance à Saint-Ouen-la-Rouërie
J0323010	−0.42	0.39	19	62	−1.6874	48.5271	775	678	213	Le Guyoult à Epiniac
J1103010	−0.82	0.61	32	103	−2.3337	48.4024	867	672	235	L'Arguenon à Jugon-les-Lacs
J1114010	−0.54	0.22	41	113	−2.2478	48.3644	775	679	199	La Rosette à Mégrit
J1313010	−0.77	0.72	40	244	−2.5686	48.4848	772	674	175	Le Gouessant à Andel
J1513010	−0.87	0.81	103	135	−2.8332	48.4474	1055	653	371	Le Gouët à Saint-Julien
J1813010	−0.68	0.57	17	342	−3.0672	48.7054	908	668	241	Le Leff à Quemper-Guézennec
J2233010	−0.74	0.62	94	265	−3.3982	48.5465	1088	644	562	Le Léguer à Belle-Isle-en-Terre
J2603010	−0.48	0.54	26	44	−3.7997	48.5660	1168	660	523	Le Jarlot à Plougonven
J2605410	−0.56	0.51	27	42	−3.7971	48.5671	1136	655	445	Le Tromorgant à Plougonven
J2723010	−0.66	0.74	13	142	−3.9242	48.5847	1175	660	641	La Penze à Taulé (Penhoat)
J3024010	−0.12	0.76	33	45	−4.0762	48.6163	966	663	489	Le Guillec à Trézilidé
J3205710	−0.13	0.91	39	24	−4.3618	48.5310	1098	673	596	L'Aber Wrac'h au Drennec
J3213020	−0.56	0.81	47	27	−4.4058	48.5240	1102	673	574	L'Aber-Benoit à Plabennec (Loc Maria)
J3323020	−0.36	0.66	20	95	−4.6805	48.4556	1058	673	468	L'Aber Ildut à Brélès (Keringar)
J3601810	−2.25	1.21	97	117	−3.6678	48.3889	1246	648	589	L'Aulne à Scrignac (Le Goask)
J3713010	−0.82	0.65	91	258	−3.5100	48.3211	1099	660	531	L'Hyères à Trébrivan (Pont Neuf)
J3834010	−0.11	0.77	26	140	−4.0610	48.2599	1289	663	765	La Douffine à Saint-Ségal (Kerbriant)
J4214510	−0.88	0.62	128	7	−3.9866	48.1025	1217	669	706	Le Langelin à Briec (Pont D 72)
J4224010	−0.52	0.64	22	108	−4.0146	47.9891	1191	682	665	Le Jet à Ergué-Gabéric
J4313010	−0.25	0.95	20	181	−4.1470	48.0269	1205	679	638	Le Steir à Guengat (Ty Planche)
J4514010	−0.39	0.66	20	21	−3.8745	47.8838	1101	699	498	Le Moros à Concarneau (Pont D 22)
J4614010	−0.72	0.65	36	72	−3.7512	47.9075	1230	680	680	Le Ster Goz à Bannalec (Pont Meya)
J4742010	−0.33	0.74	23	576	−3.4691	47.9038	1192	666	548	L'Éllé à Arzano (Pont Ty Nadan)
J4803010	−1.29	1.14	100	102	−3.6705	47.9883	1295	662	720	L'Isole à Scaër (Stang Boudilin)
J4902010	−0.06	0.90	7	832	−3.5429	47.8677	1203	668	564	La Laïta à Quimperlé (ancienne)
J5102210	−0.54	0.54	24	299	−3.4197	47.9054	1194	674	534	Le Scorff à Plouay (Pont Kerlo)
J5613010	−0.53	0.52	44	316	−2.9741	47.9013	941	687	338	L'Evel à Guénin
J5704810	−0.73	0.50	46	46	−3.2011	47.9051	1146	687	568	Le Coët-Organ à Quistinic (Kerdec)
J6213010	−0.51	1.05	25	182	−2.9895	47.7221	1021	698	473	Le Loch à Brech
J7083110	−0.40	0.62	44	152	−1.4982	48.1832	838	693	227	Le Chevré à la Bouëxière (Le Drugeon)
J7483010	−0.32	0.75	17	809	−1.7225	48.0199	748	710	185	La Seiche à Bruz (Carcé)
J7633010	−0.24	0.89	24	406	−1.6299	47.8601	779	709	231	Le Semnon à Bain-de-Bretagne (Rochereuil)
J7824010	−0.26	0.76	15	112	−1.6910	47.7130	780	712	202	L'Aron à Grand-Fougeray (La Bernardais)
J7973010	−0.20	0.90	27	40	−1.9791	47.7766	773	716	237	Le Canut Sud à Saint-Just (La rivière Colombel)
J8002310	−1.58	1.12	178	29	−2.9654	48.3216	1105	649	404	L'Oust à Saint-Martin-des-Prés (La Ville Rouault)
J8363110	−0.44	0.79	35	301	−2.3687	47.9948	807	682	236	L'Yvel à Loyat (Pont D 129)
J8433010	−0.49	0.72	49	135	−2.7029	47.8259	993	691	408	La Claie à Saint-Jean-Brévelay
J8602410	−0.38	0.57	69	28	−2.1435	47.9829	856	664	262	L'Aff à Paimpont (Pont du Secret)
J8632410	−0.37	0.68	14	343	−2.0744	47.8297	815	686	245	L'Aff à Quelneuc (La rivière)
J8813010	−0.42	0.90	26	161	−2.4321	47.7174	1009	698	439	L'Arz à Molac (Le Qinquizio)
J9300610	−0.10	0.54	1	10 148	−2.1255	47.5801	819	701	231	La Vilaine à Rieux

Table C4. Continued.

Catchment code	e_{Q/E_p}	$e_{Q/P}$	Altitude of the outlet (m a.s.l.)	Area (km^2)	X outlet (DD)	Y outlet (DD)	Long-term precipitation P ($mm\,yr^{-1}$)	Long-term potential evaporation E ($mm\,yr^{-1}$)	Long-term streamflow Q ($mm\,yr^{-1}$)	River name
K0010010	0.42	1.48	1116	60	4.1475	44.7704	1369	558	1374	La Loire à Usclades-et-Rieutord (Rieutord)
K0403010	−0.07	1.02	936	138	4.3015	45.0575	1097	579	699	Le Lignon du Velay au Chambon-sur-Lignon
K0454010	−0.19	0.79	596	217	4.2141	45.2146	941	612	454	La Dunières à Sainte-Sigolène (Vaubarlet)
K0523010	−1.02	0.38	706	347	3.9380	45.3071	1114	585	378	L'Ance du Nord à Saint-Julien-d'Ance (Laprat)
K0567520	−0.48	0.86	653	129	4.2494	45.3148	951	619	454	La Semène à Saint-Didier-en-Velay (Le Crouzet)
K0567530	−0.07	0.36	811	58	4.3649	45.3002	1001	606	461	La Semène à Jonzieux
K0624510	−0.28	0.56	432	105	4.1870	45.4706	953	654	246	Le Bonson à Saint-Marcellin-en-Forez (Le Bled)
K0663310	−0.84	1.07	583	61	4.5258	45.6283	888	677	318	La Coise à Larajasse (Le Nézel)
K0673310	−0.15	1.05	436	181	4.3750	45.6087	883	683	268	La Coise à Saint-Médard-en-Forez (Moulin Brûlé)
K0724510	−0.53	0.65	342	13	4.2294	45.7759	768	717	204	Le Chanasson à Civens (La rivière)
K0733220	−1.58	0.63	817	60	3.8672	45.6968	1124	561	857	Le Lignon de Chalmazel à Chalmazel (Chevelières)
K0773220	−1.15	0.74	333	662	4.1649	45.7311	923	654	347	Le Lignon de Chalmazel à Poncins (2)
K0813020	−1.84	1.58	378	197	4.0022	45.8317	987	635	445	L'Aix à Saint-Germain-Laval
K0974010	−0.38	0.84	364	86	4.1866	45.9548	896	698	290	Le Gand à Neaux
K0983010	−0.47	0.84	293	435	4.1190	45.9802	932	699	363	Le Rhins à Saint-Cyr-de-Favières (Pont Mordon)
K1084010	−1.58	0.71	357	23	3.8847	46.1375	840	686	400	La Teyssonne à Changy (La Noaillerie)
K1173210	5.89	2.39	241	593	4.0495	46.3583	911	702	278	L'Arconce à Montceaux-l'Étoile
K1284810	−0.63	0.78	318	135	4.1977	47.0039	1211	657	690	La Selle à la Celle-en-Morvan (Polroy)
K1321810	−1.25	0.49	268	1792	4.1924	46.8510	998	679	368	L'Arroux à Étang-sur-Arroux (Pont du Tacot)
K1503010	−1.69	0.47	361	157	3.6812	46.1266	1113	642	458	La Besbre à Châtel-Montagne
K1524010	−0.99	0.69	314	121	3.6880	46.1940	999	686	436	Le Barbenan au Breuil
K1724210	−1.05	0.80	212	114	3.7638	46.9112	1109	689	481	La Dragne à Vandenesse
K1753110	−0.91	0.25	200	333	3.6794	46.8447	978	691	398	L'Alène à Cercy-la-Tour (Coueron)
K1914510	−0.62	0.63	196	115	3.3367	46.9625	928	689	326	L'Ixeure à la Fermeté
K1954010	−0.68	0.64	207	226	3.2529	47.1341	941	686	312	La Nièvre d'Arzembouy à Poiseux (Poisson)
K2064010	−0.86	1.28	910	66	3.8584	44.7298	938	562	661	Le Langouyrou à Langogne
K2123010	−0.66	0.89	1124	125	3.6993	44.6725	959	550	366	Le Chapeauroux à Châteauneuf-de-Randon (Hermet)
K2233020	−0.35	1.37	634	231	3.6368	44.9674	867	568	349	L'Ance du Sud à Monistrol-d'Allier (Pouzas)
K2514010	−0.08	1.13	768	156	3.0065	45.1340	1223	563	542	L'Allanche à Joursac (Pont du Vernet)
K2523010	−0.06	0.93	710	322	3.0271	45.1591	1191	560	601	L'Alagnon à Joursac (Le Vialard)
K2834010	−0.38	0.83	836	71	3.6289	45.4470	1091	579	475	La Dolore à Saint-Bonnet-le-Chastel (Moulin Neuf)
K2871910	−1.12	0.56	412	795	3.6102	45.6893	1059	607	389	La Dore à Saint-Gervais-sous-Meymont (Maison du Parc/Giroux-Dore)
K2884010	−2.87	0.74	403	73	3.5938	45.7020	1103	611	641	La Faye à Olliergues (Giroux-Faye)
K2944010	−1.66	0.65	335	72	3.5665	45.7455	1043	633	526	Le Couzon à Courpière (Le Salet)
K3206010	−3.04	−0.31	784	8	2.8933	45.7608	1145	609	957	La source-de-chez-Pierre à Ceyssat
K3222010	−0.70	0.68	666	360	2.8490	45.8330	1128	609	513	La Sioule à Pontgibaud
K3264010	−0.57	0.70	538	111	2.6741	45.8705	936	650	259	La Saunade à Pontaumur
K3292020	−0.74	0.65	502	1300	2.7961	45.9735	1001	634	389	La Sioule à Saint-Priest-des-Champs (Fades-Besserve)
K4094010	−0.50	0.41	153	478	2.9986	47.3553	846	697	207	Le Nohain à Saint-Martin-sur-Nohain (Villiers)
K4443010	−0.30	0.59	79	165	1.6631	47.7609	738	718	94	L'Ardoux à Lailly-en-Val
K4873110	−0.01	0.56	82	263	0.8973	47.5669	674	709	156	La Brenne à Villedômer (Bas-Villaumay)
K5090910	−0.21	0.69	321	526	2.5491	46.1767	901	673	350	Le Cher à Chambonchard
K5183010	−0.41	0.54	329	861	2.4455	46.1841	959	680	306	La Tardes à Évaux-les-Bains
K6334010	−0.54	0.01	180	79	2.4362	47.4912	866	699	215	La Nère à Aubigny-sur-Nère
K6402510	−0.80	0.06	102	1240	2.0332	47.4234	829	702	229	La Sauldre à Salbris
K6492510	−0.85	0.30	73	2297	1.5355	47.2870	780	710	187	La Sauldre à Selles-sur-Cher
K7312610	−0.90	0.65	82	1707	1.1265	47.0171	796	726	227	L'Indre à Saint-Cyran-du-Jambot
K7414010	−0.47	0.60	99	109	1.2412	47.1361	729	724	177	La Tourmente à Villeloin-Coulangé (Coulangé)
K7424010	−0.30	0.51	97	78	1.2112	47.1826	725	722	151	L'Olivet à Beaumont-Village (1)
K7514010	−0.20	0.69	66	128	0.8187	47.2474	670	732	138	L'Échandon à Saint-Branchs

Table C5. Continued.

Catchment code	e_{Q/E_p}	$e_{Q/P}$	Altitude of the outlet (m a.s.l.)	Area (km^2)	X outlet (DD)	Y outlet (DD)	Long-term precipitation P ($mm\,yr^{-1}$)	Long-term potential evaporation E ($mm\,yr^{-1}$)	Long-term streamflow Q ($mm\,yr^{-1}$)	River name
L0010610	−1.15	0.68	749	64	2.0067	45.7014	1397	611	845	La Vienne à Peyrelevade (Servières)
L0010620	−1.43	0.68	740	77	1.9952	45.6996	1391	611	771	La Vienne à Peyrelevade (La Rigole du Diable)
L0093010	−0.27	0.96	301	188	1.5538	45.7666	1200	702	624	La Combade à Masléon
L0314010	−0.95	0.71	313	131	1.5782	45.9557	1145	703	603	La Vige à Saint-Martin-Sainte-Catherine
L0563010	−0.77	0.72	218	605	1.2404	45.7568	1113	723	398	La Briance à Condat-sur-Vienne (Chambon Veyrinas)
L0624010	−0.45	0.76	230	153	1.1308	45.7719	1075	729	345	L'Aixette à Aixe-sur-Vienne
L0813010	−0.59	0.76	214	298	0.9150	45.9133	1051	730	404	La Glane à Saint-Junien (Le Dérot)
L4033010	−0.53	0.84	448	190	2.1768	45.9321	1121	651	414	La Rozeille à Moutier-Rozeille (Aubusson)
L4220710	−0.67	0.60	215	1235	1.6789	46.3783	1062	679	381	La Creuse à Fresselines
L4321710	−0.62	0.49	272	561	1.9950	46.3572	916	695	282	La Petite Creuse à Genouillac
L4411710	−0.59	0.57	218	853	1.6892	46.3856	917	701	296	La Petite Creuse à Fresselines (Puy Rageaud)
L4530710	−0.73	0.54	187	2427	1.6129	46.4544	993	692	335	La Creuse à Éguzon-Chantôme
L4653010	−0.63	0.60	124	438	1.6271	46.6659	834	727	212	La Bouzanne à Velles (Forges)
L5034010	−1.37	0.52	324	129	1.4948	46.0964	1100	710	413	L'Ardour à Folles (Forgefer)
L5101810	−0.64	0.59	297	568	1.4337	46.1139	1034	705	432	La Gartempe à Folles (Bessines)
L5134010	−0.57	1.00	200	175	1.1418	46.1508	970	719	348	La Semme à Droux
L5223020	−0.44	0.75	178	286	1.0205	46.1342	1058	726	387	Le Vincou à Bellac (2)
L5323010	−0.39	0.65	171	232	0.9982	46.2518	951	737	292	La Brame à Oradour-Saint-Genest
L5623010	−0.72	1.01	183	188	1.2582	46.3553	956	723	305	La Benaize à Jouac
L6202030	−0.56	0.48	58	886	0.8178	46.9073	766	742	142	La Claise au Grand-Pressigny (Étableau 2)
M0050620	−0.08	0.71	124	909	−0.0231	48.3867	798	677	232	La Sarthe à Saint-Céneri-le-Gérei (Moulin du Désert)
M0250610	−0.13	0.73	48	2713	0.2064	48.0898	791	690	238	La Sarthe à Neuville-sur-Sarthe (Montreuil)
M0361510	−0.15	0.43	102	833	0.8133	48.3187	775	674	236	L'Huisne à Nogent-le-Rotrou (Pont de bois)
M0500610	0.03	0.55	38	5452	0.1439	47.9132	769	694	210	La Sarthe à Spay (amont)
M0680610	−0.16	0.64	21	7523	−0.3842	47.7986	761	702	204	La Sarthe à Saint-Denis-d'Anjou (Beffes)
M1034020	0.05	0.71	126	267	1.3479	48.2084	703	680	166	L'Ozanne à Trizay-lès-Bonneval (Prémoteux)
M1041610	−0.11	0.89	118	1080	1.4175	48.1514	665	683	101	Le Loir à Saint-Maur-sur-le-Loir
M1214010	−0.13	0.33	121	87	0.8492	48.0538	718	695	182	Le Couëtron à Souday (Glatigny)
M3253110	−0.79	0.97	94	185	−0.6269	48.2696	851	681	318	L'Aron à Moulay
M3313010	−1.12	0.69	115	121	−0.9454	48.2972	892	672	322	L'Ernée à Ernée
M3323010	−0.66	0.76	67	376	−0.7785	48.1676	880	680	327	L'Ernée à Andouillé (Les Vaugeois)
M3340910	−0.25	0.88	45	2908	−0.7399	48.0130	884	671	324	La Mayenne à l' Huisserie (Bonne)
M3423010	−0.24	0.78	50	404	−0.7062	48.0336	803	703	246	La Jouanne à Forcé
M3504010	−0.55	0.83	51	234	−0.7826	47.9875	827	695	247	Le Vicoin à Nuillé-sur-Vicoin
M3600910	−0.26	0.96	27	3935	−0.6992	47.8187	859	680	296	La Mayenne à Château-Gontier
M3630910	−0.08	0.87	20	4166	−0.6858	47.6787	852	682	306	La Mayenne à Chambellay
M3774010	−0.60	0.76	43	77	−0.9857	47.7839	751	709	212	Le Chéran à la Boissière
M5102010	−0.23	0.87	46	259	−0.3745	47.1931	694	740	129	Le Layon à Saint-Georges-sur-Layon
M5222010	−0.26	0.79	20	927	−0.6323	47.3164	680	741	136	Le Layon à Saint-Lambert-du-Lattay (Pont de Bézigon)
M6014010	−0.14	0.78	70	38	−0.9626	47.1778	750	734	241	Le Beuvron à Andrezé (Tuvache)
M6333020	−0.32	0.67	6	463	−1.4809	47.4635	768	725	190	L'Erdre à Nort-sur-Erdre (Moulin de Vault)
M7112410	−0.54	0.63	50	872	−1.1147	47.0184	916	725	327	La Sèvre Nantaise à Tiffauges (La Moulinette)
M7453010	−0.67	0.60	19	595	−1.3701	47.0555	877	737	273	La Maine à Remouillé
M8205020	−0.02	1.11	6	139	−1.5331	47.1222	820	745	290	L'Ognon aux Sorinières (Villeneuve)
N3001610	−0.30	0.69	65	131	−0.9509	46.7504	943	732	353	Le Grand Lay à Saint-Prouant (Monsireigne)
N3024010	−0.52	0.52	42	121	−0.9708	46.6697	911	739	302	Le Louing à Chantonnay (St-Philbert du Pont Charrault)
O0015310	1.36	1.32	558	36	0.7480	42.8668	1359	568	1154	Le Maudan à Fos
O0105110	−2.23	−0.18	2154	5	0.1183	42.8197	1641	387	1339	La Neste de Cap de Long à Aragnouet (Les Edelweiss)
O0126210	−1.31	0.90	1070	67	0.3000	42.7918	1585	461	952	La Neste de Rioumajou à Tramezaïgues (Maison Blanche)
O0362510	−0.82	0.62	472	385	1.2137	42.9087	1530	614	1263	Le Salat à Soueix-Rogalle (Kercabanac)

Table C6. Continued.

Catchment code	e_{Q/E_p}	$e_{Q/P}$	Altitude of the outlet (m a.s.l.)	Area (km^2)	X outlet (DD)	Y outlet (DD)	Long-term precipitation P ($mm\,yr^{-1}$)	Long-term potential evaporation E ($mm\,yr^{-1}$)	Long-term streamflow Q ($mm\,yr^{-1}$)	River name
O0384010	−1.10	0.52	501	170	1.2322	42.8990	1448	656	1067	L'Arac à Soulan (Freychet)
O0502520	−1.18	0.61	386	1159	1.1411	42.9914	1411	655	903	Le Salat à Saint-Lizier (Saint Girons)
O0525010	0.02	1.16	441	14	1.0504	43.0003	1054	742	958	La Gouarège à Cazavet (Aliou)
O0592510	−0.45	0.72	270	1579	0.9745	43.1548	1287	684	784	Le Salat à Roquefort-sur-Garonne
O0744030	−0.84	0.86	290	220	1.3599	43.0826	1070	754	531	L'Arize au Mas-d'Azil
O1115010	−0.79	0.93	1239	24	1.4161	42.7094	1530	496	1653	L'Artigue à Auzat (Cibelle)
O1432930	−0.71	0.39	521	134	1.9263	42.8931	1222	657	444	L'Hers à Bélesta (source de Fontestorbes)
O1442910	−0.81	0.73	417	191	1.9356	42.9543	1147	687	615	L'Hers Vif au Peyrat
O1484310	−1.10	1.01	507	68	1.8514	42.9404	1145	684	795	La Touyre à Lavelanet (2)
O1494330	−1.03	0.96	387	95	1.9121	42.9892	1086	709	638	La Touyre à Léran
O1584610	−0.44	0.69	306	136	1.7733	43.0434	959	775	351	Le Douctouyre à Vira (Engraviès)
O1634010	−0.35	0.65	239	197	1.7497	43.2014	761	816	179	La Vixiège à Belpech
O2344010	−0.50	0.71	122	524	1.4339	43.7528	758	822	120	Le Girou à Cépet
O2725010	−0.17	0.61	191	36	0.7293	43.4974	723	799	165	La Lauze à Sémézies-Cachan (Faget-Abbatial)
O3006710	−0.59	0.83	1026	10	3.7890	44.3403	1634	564	1457	La Goudech à Saint-Maurice-de-Ventalon (La Cépède)
O3011010	−0.43	0.73	927	65	3.7545	44.3615	1660	564	1552	Le Tarn au Pont-de-Montvert (Fontchalettes)
O3035210	1.48	0.88	611	26	3.6127	44.3560	1231	627	633	Le Briançon aux Bondons (Cocures)
O3064010	−0.51	1.68	554	132	3.5980	44.3148	962	641	835	Le Tarnon à Florac
O3084320	1.00	1.13	556	126	3.6030	44.3157	1500	651	863	La Mimente à Florac
O3165010	−0.59	1.64	708	34	3.4375	44.1790	1006	603	855	La Brèze à Meyrueis
O3194010	0.34	1.45	704	98	3.4263	44.1809	1019	608	630	La Jonte à Meyrueis (aval)
O3364010	−0.74	0.77	446	428	3.2895	44.0724	1208	667	505	La Dourbie à Nant (Pont de Gardies)
O3401010	−0.27	0.98	355	2143	3.0740	44.0921	1139	656	675	Le Tarn à Millau (2)
O3424010	−1.23	0.49	343	169	2.9865	44.0801	1017	728	427	Le Cernon à Saint-Georges-de-Luzençon (aval)
O3454310	0.02	0.45	340	112	2.9217	44.0813	977	686	398	La Muze à Montjaux (Saint-Hippolyte)
O4194310	−0.23	0.40	357	207	2.4172	43.6828	1174	710	645	Le Gijou à Vabre (Rocalé)
O4704030	−0.61	0.63	427	71	2.4410	43.8221	1160	722	569	Le Dadou à Paulinet (Saint-Jean-de-Jeanne)
O5042510	−0.95	0.34	578	300	2.8460	44.3991	1048	684	315	L'Aveyron à Palmas (Pont de Manson)
O5055010	−0.56	0.47	584	108	2.8712	44.4152	1103	696	279	Le Serre à Coussergues (Resuenhe)
O5092520	−1.22	0.46	533	584	2.6213	44.3622	1046	695	309	L'Aveyron à Onet-le-Château (Rodez)
O5192520	−0.80	0.51	276	1060	2.0548	44.3478	1019	710	344	L'Aveyron à Villefranche-de-Rouergue (Recoules)
O5224010	−0.29	0.74	276	208	2.0497	44.3568	958	748	357	L'Alzou à Villefranche-de-Rouergue (barrage Cabal)
O5284310	−0.94	0.59	317	104	2.0442	44.2093	953	744	329	La Serène à Saint-André-de-Najac (Canabral)
O5292510	−0.75	0.56	163	1604	1.9733	44.1515	990	726	314	L'Aveyron à Laguépie (1)
O5312910	−0.24	0.94	730	139	2.8013	44.3085	1009	666	522	Le Viaur à Arques
O5344010	−0.11	0.84	814	57	2.8130	44.2104	1019	659	534	Le Vioulou à Salles-Curan (Trébons-Bas)
O5424010	−1.13	0.42	352	161	2.4067	44.1431	999	708	362	Le Céor à Centrès (Estrebaldie)
O5464310	−1.23	0.43	363	176	2.4353	44.1080	980	723	339	Le Giffou à Saint-Just-sur-Viaur (La Fabrèguerie)
O5534010	−0.80	0.95	245	223	2.1981	44.1637	972	732	364	Le Lézert à Saint-Julien-du-Puy (Port de la Besse)
O5685010	−0.43	0.35	139	181	1.7483	44.1721	908	779	191	La Bonnette à Saint-Antonin-Noble-Val
O5754020	−0.53	0.60	125	310	1.6726	44.0242	827	800	189	La Vère à Bruniquel (La Gauterie)
O6125010	−0.08	0.90	143	62	1.1903	44.3340	825	796	264	La Petite Barguelonne à Montcuq
O6134010	−0.30	0.75	74	453	0.9963	44.1691	798	803	182	La Barguelonne à Valence (Fourquet)
O6793310	−0.16	0.58	58	834	0.2463	44.0754	816	811	160	La Gélise à Mézin (Courbian)
O6804630	−0.43	0.87	245	9	0.3240	43.3989	872	783	281	L'Osse à Castex (Mielan)
O7011510	−0.85	0.90	813	187	3.5964	44.5262	1104	564	602	Le Lot à Sainte-Hélène
O7015810	−0.57	−0.64	981	33	3.6181	44.5412	960	546	448	L'Esclancide à Pelouse (Les Salces)
O7041510	−1.22	0.71	667	468	3.4233	44.4813	1099	589	477	Le Lot à Balsièges (Bramonas)
O7085010	−0.56	−0.52	663	83	3.3114	44.5507	1013	607	314	Le Coulagnet à Marvejols
O7101510	−0.94	0.64	525	1158	3.1979	44.4428	1030	606	362	Le Lot à Banassac (La Mothe)
O7131510	−0.70	0.54	388	1633	2.8670	44.5033	1045	621	420	Le Lot à Lassouts (Castelnau)
O7145220	0.62	0.91	439	53	2.8484	44.5322	1316	607	1005	La Boralde de Saint-Chély à Castelnau-de-Mandailles

Table C7. Continued.

Catchment code	e_{Q/E_p}	$e_{Q/P}$	Altitude of the outlet (m a.s.l.)	Area (km^2)	X outlet (DD)	Y outlet (DD)	Long-term precipitation P ($mm\,yr^{-1}$)	Long-term potential evaporation E ($mm\,yr^{-1}$)	Long-term streamflow Q ($mm\,yr^{-1}$)	River name
O7234010	−0.46	0.81	948	117	3.3215	44.7664	1044	590	450	La Rimeize à Rimeize
O7245010	−0.08	0.83	947	65	3.2954	44.7919	1006	599	374	Le Chapouillet à Rimeize (Chassignoles)
O7265010	−0.60	0.67	921	78	3.3609	44.7778	929	568	384	La Limagnole à Fontans (Saint-Alban)
O7444010	−0.78	1.13	924	286	3.0850	44.8268	1051	570	787	Le Bès à Saint-Juéry
O7502510	−0.43	0.70	704	1795	3.0736	44.9231	937	589	412	La Truyère à Neuvéglise (Grandval)
O7635010	−1.08	0.87	645	109	2.6843	44.8270	1601	606	935	La Bromme à Brommat
O7874010	−1.22	0.33	236	545	2.4009	44.5873	1063	742	376	Le Dourdou à Conques
O8113510	−0.11	0.59	183	681	1.9843	44.5886	1200	732	567	Le Célé à Figeac (Merlançon)
O8133520	−0.62	1.20	142	1246	1.6793	44.5197	1107	751	446	Le Célé à Orniac (Les Amis du Célé)
O8255010	−0.92	0.80	103	119	1.2320	44.5108	914	779	328	Le Vert à Labastide-du-Vert (Les Campagnes)
O8394310	−0.64	0.45	87	220	0.9460	44.5363	892	781	159	La Lémance à Cuzorn
O9196210	−0.07	0.42	53	10	−0.0747	44.5240	804	805	114	La Cadanne à Pondaurat
P0010010	−2.40	0.65	786	89	2.6892	45.6042	1313	551	1253	La Dordogne à Saint-Sauves-d'Auvergne
P0115010	−0.30	0.89	905	21	2.6964	45.5286	1451	537	1501	La Burande à la Tour-d'Auvergne
P0115020	−0.50	0.94	569	85	2.5416	45.5425	1382	583	1038	La Burande (ou ru de Burons) à Singles
P0212510	−0.84	0.68	954	40	2.8297	45.4084	1602	552	1317	La Rhue à Égliseneuve-d'Entraigues
P0364010	−0.63	0.95	709	169	2.7512	45.3341	1302	559	765	La Santoire à Condat (Roche-Pointue)
P0885010	−1.74	0.61	377	117	2.3877	45.2970	1385	610	910	Le Mars à Bassignac (Vendes)
P0924010	−0.96	0.64	631	79	2.2395	45.4913	1286	639	708	La Triouzoune à Saint-Angel
P1114010	−0.48	0.61	566	81	2.1513	45.4687	1312	634	785	La Luzège à Maussac (Pont de Maussac)
P1154010	−1.11	0.83	452	250	2.1286	45.3823	1351	649	765	La Luzège à Lamazière-Basse (Pont de Bouyges)
P1502510	−0.52	1.02	419	455	2.1932	45.0820	1409	644	942	La Maronne à Pleaux (Enchanet)
P1772910	−1.07	0.72	559	349	2.3506	44.8815	1622	607	976	La Cère à Sansac-de-Marmiesse
P2114010	−2.05	0.67	131	63	1.7245	44.9886	1245	731	468	La Sourdoire à la Chapelle-aux-Saints
P2184310	−0.68	0.67	114	191	1.6679	44.9469	1069	768	340	La Tourmente à Saint-Denis-lès-Martel
P2484010	−0.48	0.41	77	573	1.1709	44.7899	916	780	166	Le Céou à Saint-Cybranet
P3001010	−1.48	0.74	773	42	2.0072	45.6285	1403	611	1041	La Vézère à Saint-Merd-les-Oussines (Maisonnial)
P3021010	−0.99	0.95	675	138	1.9227	45.6030	1389	623	929	La Vézère à Bugeat
P3234010	−1.57	0.56	153	104	1.4150	45.3067	1176	726	487	La Loyre à Voutezac (Pont de l'Aumonerie)
P3245010	−1.03	0.47	123	52	1.3965	45.2706	1086	748	396	Le Mayne à Saint-Cyr-la-Roche
P3352510	−0.86	0.37	478	164	1.8900	45.3771	1423	641	1047	La Corrèze à Corrèze (Pont de Neupont)
P3502510	−1.06	0.72	224	354	1.7799	45.2750	1379	668	887	La Corrèze à Tulle (Pont des soldats)
P3614010	−0.47	0.67	546	42	1.9387	45.3422	1418	670	891	La Montane à Eyrein (Pont du Geai)
P3922510	−0.42	0.81	103	954	1.5013	45.1626	1296	702	655	La Corrèze à Brive-la-Gaillarde (Le Prieur)
P4015010	−1.38	0.75	133	58	1.4680	45.0948	1076	765	461	La Couze à Chasteaux (Le Soulier)
P4271010	−0.56	0.66	56	3657	0.9584	44.9034	1157	729	496	La Vézère à Campagne
P5404010	−0.27	0.65	36	74	0.3665	44.8882	885	800	217	L'Eyraud à la Force (Bitarel)
P6081510	−0.85	0.75	137	448	0.9492	45.3766	1102	738	399	L'Isle à Corgnac-sur-l'Isle
P6134010	−0.54	0.56	154	197	1.0674	45.3438	1104	741	451	La Loue à Saint-Médard-d'Excideuil
P7001510	−0.80	0.78	91	1859	0.8046	45.2028	1061	749	408	L'Isle à Bassilac (Charrieras)
P7181510	0.26	0.49	36	3342	0.2473	45.0291	992	766	388	L'Isle à Saint-Laurent-des-Hommes (Bénévent)
P7261510	−0.59	0.50	7	3757	−0.1254	45.0214	974	769	297	L'Isle à Abzac
P8012510	−0.98	1.04	160	140	0.7524	45.5152	1100	733	478	La Dronne à Saint-Pardoux-la-Rivière (Le Manet)
P8215010	−0.59	0.45	113	40	0.4667	45.4478	969	764	230	La Belle à Mareuil
P8312520	−0.66	1.12	37	1912	0.1515	45.2387	955	767	316	La Dronne à Bonnes
Q0115710	−1.15	1.52	505	32	0.1030	43.0898	1360	710	883	L'Oussouet à Trébons
Q0214010	−1.81	0.91	337	78	0.0223	43.1753	1247	765	486	L'Échez à Louey
Q0280030	−1.75	0.90	167	876	0.0290	43.4982	1161	713	469	L'Adour à Estirac
Q0664010	−0.28	0.38	141	207	0.1244	43.5550	875	797	240	Le Bouès à Juillac
Q1094010	−0.27	1.24	92	426	−0.2346	43.6469	1030	805	332	Le Larcis à Lannux
Q1100010	−0.35	0.91	80	2921	−0.2619	43.7038	1038	772	373	L'Adour à Aire-sur-l'Adour (2)
Q2593310	−0.64	1.07	26	2478	−0.6595	43.9076	909	813	231	La Midouze à Campagne
Q3120010	−0.33	0.83	6	7707	−1.0001	43.7331	1000	799	339	L'Adour à Saint-Vincent-de-Paul
Q3464010	−0.90	0.96	6	1144	−1.0427	43.6769	1110	823	424	Le Luy à Saint-Pandelon
Q7322510	−3.30	0.85	123	498	−0.8747	43.2466	1766	717	1383	Le Saison à Mauléon-Licharre
Q8032510	−0.75	0.77	43	246	−1.0286	43.3337	1521	791	602	La Bidouze à Aïcirits-Camou-Suhast (Saint-Palais)
Q8345910	−0.33	0.75	37	17	−1.3096	43.4109	1380	825	863	Le Mendialçu à Hasparren
Q9164610	−1.89	1.09	149	157	−1.3370	43.1842	1742	731	1228	La Nive des Aldudes à Saint-Étienne-de-Baïgorry

Table C8. Continued.

Catchment code	e_{Q/E_p}	$e_{Q/P}$	Altitude of the outlet (m a.s.l.)	Area (km^2)	X outlet (DD)	Y outlet (DD)	Long-term precipitation P ($mm\,yr^{-1}$)	Long-term potential evaporation E ($mm\,yr^{-1}$)	Long-term streamflow Q ($mm\,yr^{-1}$)	River name
R1132510	−1.23	1.34	217	139	0.6898	45.7267	1059	730	448	La Tardoire à Maisonnais-sur-Tardoire
R1264001	−0.25	0.42	106	293	0.4729	45.6072	1049	754	406	Le Bandiat à Feuillade
S2224610	−0.42	0.59	41	113	−0.7528	44.4107	1023	796	260	Le Grand Arriou à Moustey (Biganon)
S2235610	−0.29	0.40	35	42	−0.7734	44.4650	927	797	183	Le Bouron à Belin-Béliet (Saint-Palais) (Moulin du Moine)
S2242510	−0.52	0.70	14	1678	−0.8711	44.5477	1017	796	292	L'Eyre à Salles
S4214010	−1.13	0.34	21	77	−1.2240	43.7808	1177	809	407	Le Magescq à Magescq
S5144010	−1.90	1.37	31	142	−1.5491	43.3215	1467	801	968	La Nivelle à Saint-Pée-sur-Nivelle
U0104010	−0.92	0.86	306	64	6.3025	48.0817	1185	646	619	Le Coney à Xertigny
U0444310	−0.72	1.41	243	225	6.2717	47.8855	1316	643	796	La Semouse à Saint-Loup-sur-Semouse
U0474010	−0.57	0.79	209	1028	6.0760	47.7488	1337	659	668	La Lanterne à Fleurey-lès-Faverney
U0610010	−0.48	0.96	195	3761	5.8257	47.5765	1105	667	492	La Saône à Ray-sur-Saône
U0635010	−0.18	0.64	200	146	5.7957	47.6062	981	674	365	La Gourgeonne à Tincey-et-Pontrebeau
U0724010	−0.92	0.93	200	385	5.6470	47.5700	968	675	373	Le Salon à Denèvre
U0924010	−0.48	0.89	232	397	5.4068	47.5784	965	666	325	La Vingeanne à Saint-Maurice-sur-Vingeanne
U0924020	−0.55	0.89	198	609	5.3672	47.4219	935	678	314	La Vingeanne à Oisilly
U1004010	−1.64	0.42	388	71	6.6680	47.8030	1894	610	1348	L'Ognon à Servance (Fourguenons)
U1025010	−0.89	0.43	445	32	6.7302	47.7314	2078	602	1640	Le Rahin à Plancher-Bas
U1054010	−0.38	0.60	229	1259	6.1813	47.4158	1299	672	583	L'Ognon à Beaumotte-Aubertans
U1074010	−0.64	0.64	200	1755	5.8260	47.2974	1247	682	489	L'Ognon à Chevigney-sur-l'Ognon
U1084010	−0.34	0.68	186	2071	5.5452	47.2929	1222	687	518	L'Ognon à Pesmes
U1109010	−0.52	0.91	291	56	5.1902	47.5840	958	665	344	La Venelle à Selongey
U1204010	−0.60	0.87	273	230	5.1248	47.5540	958	666	379	La Tille à Crécey-sur-Tille
U1224010	−0.28	0.66	223	845	5.1896	47.3734	936	672	272	La Tille à Arceau (Arcelot)
U1224020	−0.44	0.50	202	882	5.2177	47.2808	931	674	241	La Tille à Cessey-sur-Tille
U1235020	−0.66	0.94	194	271	5.2207	47.2385	829	703	305	La Norges à Genlis
U1420010	−0.39	0.79	173	11 693	5.1509	47.0674	1031	683	420	La Saône à Pagny-la-Ville (Lechatelet)
U2002010	−0.46	0.70	938	33	6.1907	46.7012	1749	537	1662	Le Doubs à Mouthe
U2012010	−0.24	0.50	855	170	6.2798	46.7730	1722	539	822	Le Doubs à Labergement-Sainte-Marie
U2022010	−0.27	0.45	824	382	6.3566	46.9063	1701	546	639	Le Doubs à la Cluse-et-Mijoux (Pontarlier amont)
U2122010	−0.51	0.68	506	1159	6.9505	47.2714	1648	554	789	Le Doubs à Goumois
U2142010	−0.44	0.67	414	1306	7.0258	47.3441	1619	560	817	Le Doubs à Glère (Courclavon)
U2215020	−0.62	0.77	394	590	6.7945	47.3055	1512	598	737	Le Dessoubre à Saint-Hippolyte
U2222010	0.02	0.84	334	2236	6.7859	47.4401	1550	580	740	Le Doubs à Mathay
U2305210	−1.28	1.10	474	9	6.9498	47.7382	1297	660	1035	Le Saint-Nicolas à Rougemont-le-Château
U2345020	−1.07	0.20	468	30	6.8285	47.7411	2155	606	1554	La Savoureuse à Giromagny
U2345030	−0.87	0.49	358	144	6.8587	47.6408	1850	642	930	La Savoureuse à Belfort
U2356610	0.00	0.21	323	43	6.7524	47.5008	1138	678	430	Le Rupt à Dung
U2425260	−0.20	0.16	275	541	6.3732	47.3381	1360	659	425	Le Cusancin à Baume-les-Dames
U2512010	−0.13	0.87	241	4658	6.0312	47.2397	1394	625	703	Le Doubs à Besançon
U2542010	−0.49	0.78	201	5169	5.5627	47.1223	1373	633	667	Le Doubs à Rochefort-sur-Nenon
U2604030	−0.69	1.84	359	291	6.2268	47.0567	1560	591	2310	La Loue à Vuillafans
U2615820	−0.28	0.53	437	210	6.0123	46.9656	1574	601	776	Le Lison (source) à Nans-sous-Sainte-Anne
U2615830	0.08	0.50	325	284	5.9576	47.0313	1533	613	816	Le Lison à Myon
U2616410	−0.10	0.42	629	15	6.0213	46.9617	1541	600	1029	Le Verneau à Nans-sous-Sainte-Anne
U2624010	−0.28	1.10	275	1068	5.9569	47.1394	1474	629	1383	La Loue à Chenecey-Buillon
U2634010	−0.28	0.98	236	1264	5.8148	47.0438	1460	636	1287	La Loue à Champagne-sur-Loue
U2722010	−0.32	0.81	180	7346	5.3510	46.9227	1360	643	760	Le Doubs à Neublans-Abergement
U3205210	−1.26	0.70	368	31	4.5583	46.2757	1034	683	517	La Grosne à Trades (Les Chambosses)
U3214010	−1.65	0.57	243	334	4.6494	46.4044	957	693	365	La Grosne à Jalogny (Cluny)
U3225010	0.87	0.78	214	271	4.5647	46.5582	901	703	226	La Guye à Sigy-le-Châtel (Corcelles)
U3424010	−0.26	0.36	176	938	5.2586	46.6740	1226	711	469	La Seille à Saint-Usuge
U4014010	−0.10	0.49	240	84	5.2900	46.1717	1023	729	199	La Reyssouze à Montagnat
U4204010	−0.53	0.65	255	41	5.1978	46.1173	1010	733	281	La Veyle à Lent
U4235010	−0.77	0.71	215	93	4.9994	46.1636	1007	736	242	Le Renon à Neuville-les-Dames
U4505010	−0.92	0.61	310	55	4.5858	46.1564	1032	694	444	L'Ardières à Beaujeu
U4624010	−0.77	0.62	211	337	4.6439	45.8744	975	708	357	L'Azergues à Châtillon

Table C9. Continued.

Catchment code	e_{Q/E_p}	$e_{Q/P}$	Altitude of the outlet (m a.s.l.)	Area (km^2)	X outlet (DD)	Y outlet (DD)	Long-term precipitation P (mm yr^{-1})	Long-term potential evaporation E (mm yr^{-1})	Long-term streamflow Q (mm yr^{-1})	River name
V0144010	0.03	0.98	606	332	6.5521	46.1136	1937	487	1827	Le Giffre à Taninges (Pressy)
V0205010	−3.49	0.20	458	28	6.4565	46.0649	1892	531	729	Le Bronze à Bonneville (Thuet)
V0245610	−0.32	0.32	436	47	6.0669	46.1397	1240	636	421	L'Aire à Saint-Julien-en-Genevois (Thairy)
V0325010	−2.93	0.70	707	171	6.6210	46.2651	1979	500	1348	La Dranse de Morzine à Seytroux (Pont de Couvaloup)
V1015010	−0.88	0.36	851	76	5.9221	46.2831	1930	535	878	La Valserine à Lélex (Niaizet)
V1015030	−1.63	0.69	579	110	5.8648	46.2200	1890	544	1214	La Valserine à Chézery-Forens (Chézery)
V1015810	−1.32	1.13	401	182	5.8006	46.1500	1712	589	1562	La Semine à Châtillon-en-Michaille (Coz)
V1214010	−7.26	0.89	528	224	6.2070	45.9053	1835	549	1336	Le Fier à Dingy-Saint-Clair
V1235210	−7.92	0.38	469	25	6.2242	45.7831	1745	586	1187	L'Ire à Doussard
V1235610	−3.62	0.24	456	93	6.2322	45.7873	1674	610	907	L'Eau Morte à Doussard
V1237410	−1.61	0.31	465	30	6.1634	45.8347	1436	618	712	Le Laudon à Saint-Jorioz
V1264010	−2.70	0.93	316	1286	5.9204	45.9013	1583	609	960	Le Fier à Vallières
V1414010	−0.26	0.20	382	158	5.6728	45.8819	1699	594	252	Le Seran à Belmont-Luthézieu (Bavosière)
V1425010	−3.11	2.23	249	41	5.6866	45.8761	1539	644	2365	Le Groin à Artemare (Cerveyrieu)
V1504010	−1.53	0.55	433	94	5.7362	45.3856	1880	565	1559	Le Guiers Mort à Saint-Laurent-du-Pont
V1774010	−0.14	0.68	204	696	5.1589	45.7150	1037	744	339	La Bourbre à Tignieu-Jameyzieu
V2024010	−1.28	0.60	793	101	6.0281	46.6400	1903	538	1045	La Saine à Foncine-le-Bas
V2035010	−0.33	0.19	819	95	5.9645	46.6069	1904	564	290	La Lemme à Fort-du-Plasne (Saint-Palais) (Pont-de-Lemme)
V2202010	−0.83	0.82	458	734	5.7669	46.6859	1752	582	1135	L'Ain à Marigny (Chalain)
V2206010	−0.43	0.79	499	51	5.7750	46.6479	1778	607	1012	Le Hérisson à Doucier
V2414010	−2.25	0.83	442	203	5.8684	46.4163	1972	544	1372	La Bienne à Saint-Claude (Chenavier)
V2444020	−0.36	0.94	323	593	5.7062	46.3627	1902	566	1568	La Bienne à Jeurre
V2814020	−0.31	0.37	272	331	5.3904	46.1123	1469	679	353	Le Suran à Neuville-sur-Ain (La Planche)
V2924010	−0.33	0.64	293	210	5.4393	45.9480	1668	606	915	L'Albarine à Saint-Rambert-en-Bugey
V2934010	0.01	0.43	242	290	5.3326	45.9545	1634	622	692	L'Albarine à Saint-Denis-en-Bugey (Pont Saint Denis)
V4144010	−0.20	0.64	309	454	4.5393	44.8748	1331	639	607	L'Eyrieux à Beauvène (Pont de Chervil)
V4214010	−0.66	0.63	542	189	5.4440	44.6191	1108	621	373	La Drôme à Luc-en-Diois
V4225010	−1.70	0.76	564	227	5.4910	44.6933	1356	568	560	Le Bez à Châtillon-en-Diois
V4275010	−0.97	0.56	329	101	5.1456	44.7747	1193	652	291	La Gervanne à Beaufort-sur-Gervanne
V4414010	−0.43	0.62	276	192	5.0159	44.6249	1028	695	303	Le Roubion à Soyans
V5045810	−1.20	1.26	638	63	3.9499	44.5755	1851	597	1267	Le Borne à Saint-Laurent-les-Bains (Pont de Nicoulaud)
V6035010	0.42	0.65	338	157	5.2141	44.2150	1000	675	247	Le Toulourenc à Malaucène (Veaux)
V6052010	−0.94	0.71	194	587	5.0690	44.2403	936	717	344	L'Ouvèze à Vaison-la-Romaine
V7124010	0.27	1.28	148	244	3.9682	44.0797	1499	755	724	Le Gardon de Mialet à Générargues (Saint-Palais) (Roucan)
W0000010	−1.37	0.32	1851	46	6.9878	45.4476	1050	260	1189	L'Isère à Val-d'Isère
W0224010	1.06	1.01	652	333	6.5847	45.4493	1289	368	1296	Le Doron de Bozel à la Perrière (Vignotan)
W2222010	0.50	1.17	750	984	5.9104	44.8174	1302	466	1026	Le Drac à Corps (Le Sautet)
W2335210	−0.23	0.85	948	70	5.8668	44.9493	1592	483	1061	La Roizonne à la Valette (La Rochette)
W2405010	0.54	0.88	885	51	5.7822	44.9142	1420	559	436	La Jonche à la Mure
W2714010	−0.04	0.66	1088	223	6.1837	45.0387	1280	325	1048	La Romanche à Mizoën (Chambon amont)
W3315010	−0.72	0.23	962	74	5.5313	45.1126	1446	569	248	Le Meaudret à Méaudre
W3335210	−1.49	0.59	707	37	5.4452	45.0043	1408	564	471	L'Adouin à Saint-Martin-en-Vercors (Saint-Palais) (Tourtre)
X0010010	0.98	1.44	1363	206	6.6791	44.9240	1176	383	739	La Durance à Val-des-Prés (Les Alberts)
X0100010	−1.39	0.83	1190	548	6.6255	44.8865	1115	381	729	La Durance à Briançon (aval)
X0310010	−1.88	0.60	784	2283	6.4878	44.5522	1038	405	678	La Durance à Embrun (La Clapière)
X0434010	1.46	1.03	1136	542	6.6525	44.3837	1001	382	555	L'Ubaye à Barcelonnette (Abattoir)
X0454010	1.26	1.27	806	943	6.4011	44.4501	997	409	661	L'Ubaye au Lauzet-Ubaye (Roche Rousse)
X0500010	−1.03	0.93	756	3580	6.2809	44.4752	1026	421	667	La Durance à Espinasses (Serre-Ponçon)
X1034020	−0.14	1.14	674	731	5.7144	44.4428	1135	581	587	Le Buech à Serres (Les Chambons)
X1225010	−0.01	0.85	829	165	6.2754	44.2170	916	539	504	Le Bes à la Javie (Esclangon-Péroure)
X2114010	0.97	0.94	943	138	6.5020	43.9961	1080	538	535	L'Issole à Saint-André-les-Alpes (Mourefrey)

Table C10. Continued.

Catchment code	e_{Q/E_p}	$e_{Q/P}$	Altitude of the outlet (m a.s.l.)	Area (km^2)	X outlet (DD)	Y outlet (DD)	Long-term precipitation P ($mm\,yr^{-1}$)	Long-term potential evaporation E ($mm\,yr^{-1}$)	Long-term streamflow Q ($mm\,yr^{-1}$)	River name
Y0115410	−1.50	0.96	101	16	2.9862	42.5255	856	861	550	La Massane à Argelès-sur-Mer (Mas d'en Tourens)
Y0255020	−0.14	0.65	197	49	2.6983	42.4946	939	817	228	L'Ample à Reynès (Le Vila)
Y0325010	0.38	0.78	160	32	2.7330	42.5986	780	846	199	La Canterrane à Terrats (Moulin d'en Canterrane)
Y0624020	−0.31	0.02	246	218	2.4977	42.8022	984	738	408	L'Agly à Saint-Paul-de-Fenouillet (Clue de la Fou)
Y1225010	0.25	0.07	346	66	2.3992	43.0601	901	775	277	Le Lauquet à Greffeil
Y1325010	−0.10	0.46	128	142	2.0908	43.2764	719	853	117	Le Treboul à Villepinte
Y1415020	−0.09	0.33	94	242	2.4314	43.2326	1043	762	343	L'Orbiel à Bouilhonnac (Villedubert)
Y1416210	−0.67	0.84	109	85	2.4375	43.2532	1013	769	296	La Clamoux à Malves-en-Minervois
Y2015010	0.63	1.21	198	155	3.6582	44.0003	1483	739	949	L'Arre au Vigan (La Terrisse)
Y2102010	−0.73	0.87	139	916	3.7346	43.9157	1389	748	615	L'Hérault à Laroque
Y2214010	−0.37	1.06	160	181	3.3234	43.7287	1296	750	771	La Lergue à Lodève
Y3204010	0.49	1.25	40	116	3.8718	43.6513	910	862	602	Le Lez à Montferrier-sur-Lez (Lavalette)
Y4002010	−0.32	0.46	252	50	5.7272	43.4876	780	819	96	L'Arc à Pourrières
Y4022010	−0.06	0.56	174	297	5.5143	43.5013	706	818	112	L'Arc à Meyreuil (Pont de Bayeux)
Y4214010	−0.46	0.19	96	205	5.1746	43.6286	637	824	82	La Touloubre à la Barben (La Savonnière)
Y4604020	0.52	0.55	81	184	6.0369	43.1941	892	828	175	Le Gapeau à Solliès-Pont
Y4624010	−0.03	0.83	12	536	6.1482	43.1488	873	857	182	Le Gapeau à Hyères (Sainte-Eulalie)
Y5005210	0.47	0.40	254	146	5.9514	43.4965	812	834	110	Le Cauron à Bras (Pont de l'Avocade)
Y5032010	−0.74	0.64	183	505	6.0247	43.5022	765	821	168	L'Argens à Châteauvert
Y5105010	3.33	1.35	181	203	6.1764	43.4420	830	849	277	Le Caramy à Vins-sur-Caramy (Les Marcounious)
Y5106610	1.22	0.86	189	228	6.2258	43.4420	851	852	159	L'Issole à Cabasse (Pont des Fées)
Y5202010	−0.73	0.72	42	1651	6.4742	43.4445	811	839	185	L'Argens aux Arcs
Y5215020	−0.34	0.92	46	229	6.4534	43.3949	852	879	258	L'Aille à Vidauban (Le Baou)
Y5235010	−0.58	0.78	151	194	6.4812	43.5063	892	767	181	La Nartuby à Trans-en-Provence
Y5235030	−0.13	0.61	235	149	6.4232	43.5778	896	741	182	La Nartuby à Châteaudouble (Rebouillon)
Y5312010	−0.95	0.69	8	2514	6.6452	43.4513	822	841	191	L'Argens à Roquebrune-sur-Argens
Y5505410	−3.86	0.72	7	48	6.8496	43.4429	825	877	239	Le Grenouiller à Saint-Raphaël (Agay)
Y5615010	−0.11	0.94	133	206	7.0088	43.6981	1112	709	488	Le Loup à Tourrettes-sur-Loup (Les Vallettes)
Y5615020	−0.06	0.79	192	153	6.9921	43.7213	1130	690	412	Le Loup à Gourdon (Loup amont)
Y6432010	−0.60	0.96	188	1829	7.1905	43.9081	1144	563	576	Le Var à Malaussène (La Mescla)
Y6434010	0.19	1.04	140	443	7.1590	43.8446	1042	706	425	L'Estéron au Broc (La Clave)
Y6624010	−0.16	1.31	280	453	7.5204	43.9316	1127	596	770	La Roya à Breil-sur-Roya

The Supplement related to this article is available online at doi:10.5194/hess-20-4503-2016-supplement.

Acknowledgements. The authors would like to acknowledge Météo-France for making the SAFRAN meteorological archive available for this study, and SCHAPI-Banque Hydro for the hydrometrical series. They would also like to acknowledge the reviews of Alberto Viglione, Francis Chiew, Tim McVicar and an anonymous reviewer, which contributed to improving this paper.

Edited by: R. Merz
Reviewed by: F. H. S. Chiew, L. Gudmundsson, and A. Viglione

References

Allen, R., Pereira, L., Raes, D., and Smith, M.: Crop evapotranspiration – Guidelines for computing crop water requirements, FAO, Rome, FAO Irrigation and Drainage paper 56, 100 pp., 1998.

Arora, V. K.: The use of the aridity index to assess climate change effect on annual runoff, J. Hydrol., 265, 164–177, 2002.

Banque Hydro portal: Hydrometric data, available at: http://www.hydro.eaufrance.fr/, last access: 30 September 2016.

Chiew, F.: Estimation of rainfall elasticity of streamflow in Australia, Hydrolog. Sci. J., 51, 613–625, 2006.

Chiew, F., Potter, N. J., Vaze, J., Petheram, C., Zhang, L., Teng, J., and Post, D. A.: Observed hydrologic non-stationarity in far south-eastern Australia: implications for modelling and prediction, Stoch. Env. Res. Risk A., 28, 3–15, doi:10.1007/s00477-013-0755-5, 2013.

Coron, L., Andréassian, V., Perrin, C., Bourqui, M., and Hendrickx, F.: On the lack of robustness of hydrologic models regarding water balance simulation: a diagnostic approach applied to three models of increasing complexity on 20 mountainous catchments, Hydrol. Earth Syst. Sci., 18, 727–746, doi:10.5194/hess-18-727-2014, 2014.

Donohue, R. J., McVicar, T. R., and Roderick, M. L.: Assessing the ability of potential evaporation formulations to capture the dynamics in evaporative demand within a changing climate, J. Hydrol., 386, 186–197, 2010.

Donohue, R. J., Roderick, M., and McVicar, T.: Assessing the differences in sensitivities of runoff to changes in climatic conditions across a large basin, J. Hydrol., 406, 234–244, 2011.

Dooge, J.: Sensitivity of runoff to climate change: a Hortonian approach, B. Am. Meteorol. Soc., 73, 2013–2024, 1992.

Efron, B. and Tibshirani, R.: An introduction to the bootstrap, CRC press, Boca Raton, 1994.

Fu, G., Charles, S. P., and Chiew, F.: A two-parameter climate elasticity of streamflow index to assess climate change effects on annual streamflow, Water Resour. Res., 43, W11419, doi:10.1029/2007WR005890, 2007a.

Fu, G., Charles, S. P., Viney, N. R., Chen, S., and Wu, J. Q.: Impacts of climate variability on stream-flow in the Yellow River, Hydrol. Process., 21, 3431–3439, 2007b.

Johnston, J.: Econometric methods, McGraw-Hill, New York, 437 pp., 1972

Lebecherel, L., Andréassian, V., and Perrin, C.: On regionalizing the Turc–Mezentsev water balance formula, Water Resour. Res., 49, 7508–7517, doi:10.1002/2013WR013575, 2013.

Le Moigne, P.: Description de l'analyse des champs de surface sur la France par le système SAFRAN, Météo France CNRM/GMME/MC2, Toulouse, 2002.

Le Moine, N., Andréassian, V., Perrin, C., and Michel, C.: How can rainfall-runoff models handle intercatchment groundwater flows? Theoretical study over 1040 French catchments, Water Resour. Res., 43, W06428, doi:10.1029/2006WR005608, 2007.

Mezentsev, V.: Back to the computation of total evaporation, Meteorologia i Gidrologia, 5, 24–26, 1955.

Nelder, J. and Mead, R.: A simplex method for function minimization, Comput. J., 7, 308–313, 1965.

Nemec, J. and Schaake, J.: Sensitivity of water resources systems to climate variation, Hydrolog. Sci. J., 27, 327–343, 1982.

Niemann, J. D. and Eltahir, A. B.: Sensitivity of regional hydrology to climate changes, with application to the Illinois River basin, Water Resour. Res., 41, W07014, doi:10.1029/2004WR003893, 2005.

Oudin, L., Hervieu, F., Michel, C., Perrin, C., Andréassian, V., Anctil, F., and Loumagne, C.: Which potential evapotranspiration input for a lumped rainfall-runoff model?: Part 2 – Towards a simple and efficient potential evapotranspiration model for rainfall-runoff modelling, J. Hydrol., 303, 290–306, 2005.

Potter, N. J. and Zhang, L.: Interannual variability of catchment water balance in Australia, J. Hydrol., 369, 120–129, 2009.

Potter, N. J., Chiew, F. H. S., and Frost, A. J.: An assessment of the severity of recent reductions in rainfall and runoff in the Murray-Darling Basin, J. Hydrol., 381, 52–64, 2010.

Potter, N. J., Petheram, C., and Zhang, L.: Sensitivity of streamflow to rainfall and temperature in south-east Australia during the Millenium drought, 19th International Congress on Modelling and Simulation (MODSIM2011), 12–16 December 2011, Perth, Australia, 2011.

Sankarasubramanian, A., Vogel, R. M., and Limbrunner, J. F.: Climate elasticity of streamflow in the United States, Water Resour. Res., 37, 1771–1781, 2001.

Schaake, J. and Liu, C.: Development and application of simple water balance models to understand the relationship between climate and water resources, New Directions for Surface Water Modeling, IAHS, Wallingford, 343–352, 1989.

Shuttleworth, W. J.: Evaporation, in: Handbook of hydrology, edited by: Maidment, D. R., McGraw-Hill, New-York, 1993.

Turc, L.: The water balance of soils: relationship between precipitations, evaporation and flow (Le bilan d'eau des sols: relation entre les précipitations, l'évaporation et l'écoulement), Ann. Agron., 5, 491–595, 1954.

Vogel, R. M., Wilson, I., and Daly, C.: Regional regression models of annual streamflow for the United States, J. Irrig. Drain. E.-ASCE, 125, 148–157, 1999.

Wolock, D. M. and McCabe, G. J.: Estimates of runoff using water-balance and atmospheric general circulation models, J. Am. Water Resour. As., 35, 1341–1350, 1999.

Yang, H. and Yang, D.: Derivation of climate elasticity of runoff to assess the effects of climate change on annual runoff, Water Resour. Res., 47, W07526, doi:10.1029/2010WR009287, 2011.

Yang, H., Yang, D., Lei, Z., and Sun, F.: New analytical derivation of the mean annual water-energy balance equation, Water Resour. Res., 44, W03410, doi:10.1029/2007WR006135, 2008.

Yang, H., Yang, D., and Hu, Q.: An error analysis of the Budyko hypothesis for assessing the contribution of climate change to runoff, Water Resour. Res., 50, 9620–9629, 2014.